CHALMERS

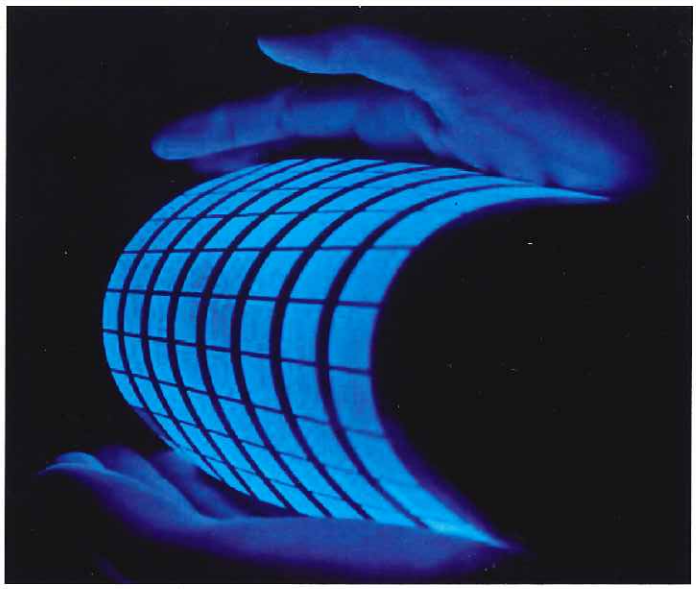

Inkjet Printing for 'Large Area Printed Organic Light-Emitting Diodes'

Master's Thesis in the Master Degree Programme, Advanced Engineering Materials

WEINA LU

Department of Materials and Manufacturing Technology
CHALMERS UNIVERSITY OF TECHNOLOGY
Göteborg, Sweden, Sep 2011

Master Thesis

INKJET PRINGTING FOR 'LARGE AREA PRINTED ORGARNIC LIGHT-EMITTING DIODES'

WEINA LU

Master Degree Programme, Advanced Engineering Materials

Department of Materials and Manufacturing Technology

CHALMERS UNIVERSITY OF TECHNOLOGY

1. Supervisor: **Dr.Maosheng Ren**

Holst Centre/TNO, High Tech Campus 31, PO Box 8550,5605 KN Eindhoven, The Netherlands

Phone: +31 (0) 40 4020536

E-mail: mao.ren@tno.nl

2. Examiner: **Shumin Wang**

Department of Microtechnology and Nanoscience

Chalmers University of Technology, 41296 Göteborg, Sweden

Phone: +46 (0) 31 772 50 39,

Fax: +46 (0)31 772 15 40

E-mail: shumin@chalmers.se

Abstract

In order to get homogeneous films with ink-jet printing and reduce the coffee stain effect, we studied the optimizations of the drying strategy and the solvent selection for the ink-jet printing process for producing OLED devices.

Experiments have been performed to study the influences of the drying temperature and drying method, and the properties of the solvents in both the single solvent system and the mixture solvent systems on coffee stain development during the drying process, related to the evaporation rate and the Marangoni effect. The results obtained reveal that the coffee stain can be reduced considerably by choosing a suitable temperature and drying method. Furthermore, by choosing the appropriate solvent or solvent mixture for a certain solute, an inward, outward or lack of Marangoni flow can be achieved which controls the coffee stain development, leading to a homogeneous layer formation.

Key words: Ink-jet printing, coffee stain, evaporation rate, Marangoni effect

Abbreviation List

OLED	Organic Light-emitting diode
LED	Light-emitting diode
LCD	Liquid Crystal Display
LEP	Light Emitting Polymer
EML	Emission Layer
ETL	Electron Transport Layer
HIL	Hole Injection Layer
HTL	Hole Transport Layer
ITO	Indium tin oxide
PEDOT:PSS	Poly(3,4-ethylenedioxythiophene) poly(styrenesulfonate)
SMOLED	Small Molecule Organic Light-emitting diode
PLED	Polymer light-emitting diodes
AMOLED	Active-matrix Organic Light-emitting diode
PMOLED	Passive-matrix Organic Light-emitting diode
IJP	Ink-jet Printing
DP	Dot pitch
LP	Line pitch
wt%	Weight percentage
v	Volume
°C	Celsius
σ_P	Surface energy of the polymer
σ_s	Surface tension of the solvent
σ_{sol}	Surface energy of the solute
σ_{HIL}	Surface energy of the HIL material
V	Voltage
Eff	Current efficiency
SxDx	Substrate x Device x

Contents

1. Introduction

Organic Light Emitting Diodes (OLED) are drawing more and more people's attention for use in the next generation of display technologies after Light Emitting Diodes (LED).

OLEDs have plenty of advantages such as: self-luminous, wide viewing angles, high contrast, better power efficiency, high response rate, full-color technology, and light weight. Because of the different manufacturing process, OLEDs are supposed to have lower cost and can be fabricated on flexible plastic substrates (Figure 1.1).

Since 2003, OLEDs have been used on PDAs, MP3 players and mobile phones which have small, portable system screens. Due to the early stage of development, these OLEDs emitted less light per unit area compared to inorganic solid-state based LED point-light sources. But the OLED display has so many advantages that cannot be achieved by the traditional Liquid Crystal Display (LCD), that the development of a new generation of display technologies is ongoing inevitably [1].

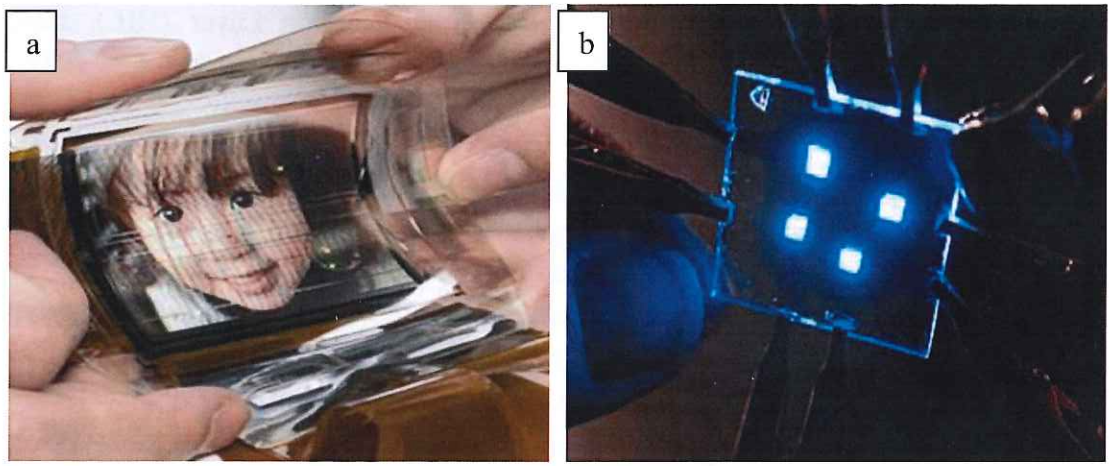

Figure 1.1 (a): Demonstration of a flexible OLED display [2]; (b): A blue-light emitting OLED device [3].

1.1 Background of the OLEDs

1.1.1 Outline

An organic light emitting diode (OLED) is a light-emitting diode (LED) in which the emissive electroluminescent layer is a film of organic compounds which emits light in response to an electric current. This layer of organic semiconductor material is situated between two electrodes [4].

The technology of OLED displays is quite different compared to the traditional Liquid Crystal Display (LCD) technology: OLEDs can function without a backlight, as the organic materials inside the OLED will light when there is a current pass through. Moreover, because a very thin coating with organic materials and a glass substrate are used, it is much thinner and lighter than an LCD.

There are two main types of OLEDs based on the light-emitting materials: the first is based on small molecules and the other one employs polymers. Polymer Light-Emitting Diodes (PLED) allow for larger display sizes and flexible substrates. OLED displays can use either passive-matrix (PMOLED) or active-matrix addressing schemes (AMOLED) [1].

1.1.2 Structure and working principle of the OLEDs

The typical structure of an OLED is composed of a thin and transparent layer of Indium Tin Oxide (ITO) connected with positive electrode and another metal cathode, packing an organic materials layer deposit between them, like a sandwich. At the beginning, the basic polymer OLEDs only consisted of a single organic layer, but now, multi-layer OLEDs can consist of two or more layers in order to improve the device efficiency. The layers of the whole structure layers include: Hole Injection Layer (HIL), Hole Transport Layer (HTL), Emission Layer (EML) and Electron Transport Layer (ETL) (Figure 1.2).

The work principle of OLEDs can be described as follows: when there is a direct current applied on the component, the voltage energy will drive electrons and holes into the emission layer (EML) from the cathode and anode. When the electron and hole combine in the emission layer, photons will be produced, and light will come out (Figure 1.3). According to different material properties, it can generate red, green or blue light; with these three primitive colors, all basic color can be constituted [1].

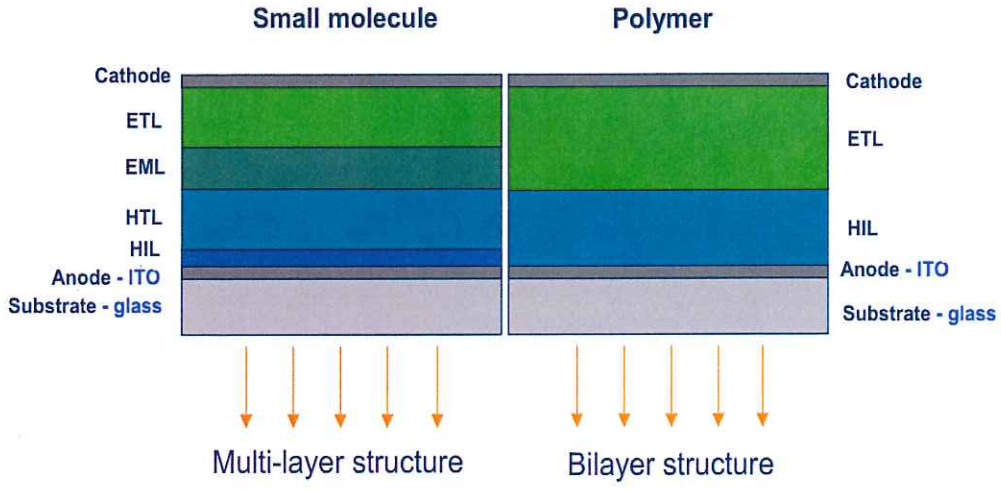

Figure 1.2 Typical layer structures of OLEDs: SMOLED and PLED [5].

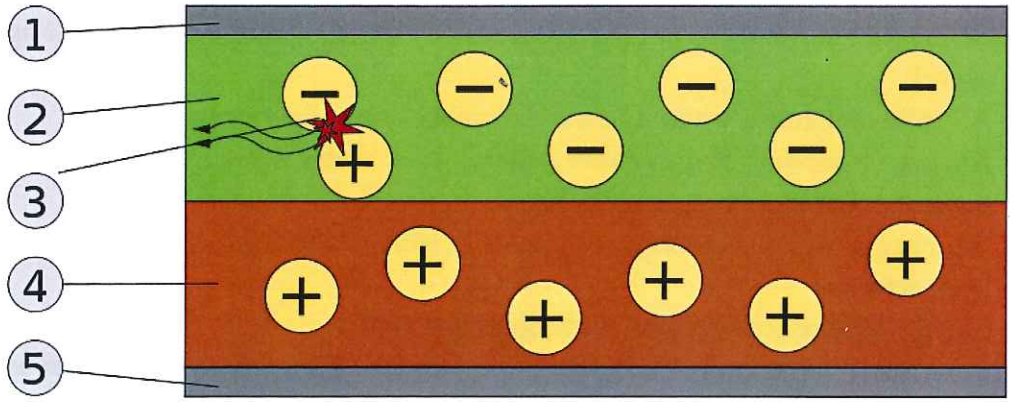

Figure 1.3 Schematic of an OLED device:1,Cathode (-); 2, Emissive layer (EL);3,Anode holes and cathode electrons combine in emissive layer, generate photons;4,Conductive layer;5,Anode [4].

1.1.3 Selection of organic light-emitting material

The properties of the organic light-emitting materials have strong influence on the device properties. In the choice of anode material, we prefer a material with high work function and translucency, so the ITO transparent conductive films are widely used for its stability and high work function. While in the choice of cathode material, in order to increase the device efficiency, metals with low work function are needed such as Ag, Al, Ca, In, Li and Mg, or a composite of them like Mg-Ag [4].

Generally, the OLEDs have two major types, depending on the light-emitting materials: OLED materials with low molecular weight called small molecules OLED (SMOLED) and polymer light-emitting diodes (PLED) based on a light-emitting polymer (LEP) [1]. Organometallic chelates (for example Alq3), fluorescent and phosphorescent dyes and conjugated dendrimers are the common used small molecules in OLEDs. However, for PLED, an electroluminescent conductive polymer that emits light when connected to an external voltage must be chosen, typical polymers include derivatives of poly (p-phenylene vinylene) and polyfluorene. The SMOLED is mainly manufactured by thermal evaporation in a vacuum, and PLED can be processed by spin coating or ink-jet printing [4].

1.1.4 Advantages and disadvantages of OLEDs

This section summarizes some of the important advantages and disadvantages of OLEDs [6].

Advantages of OLEDs:

- The thickness of an OLED layer is 1/200 of human hair, and the thickness of an OLED screen is only 1/3 of the thickness of an LCD screen, so it is much lighter as well.
- All solid structures, without liquid: better shakeproof performance.
- Almost no viewing angle problem exists: even under a large viewing angle, the screen performance is still not affected.
- High response rate, the response time is 1/1000 of the response time of standard LCD screens.
- Lower working temperature, down to minus 40 ℃.
- Lower cost in the future due to the improvement of the simple process methods.
- Higher light efficiency and much brighter.
- More flexible on selection of substrates, can be fabricated on flexible plastic substrates.

Disadvantages of OLEDs:

- Short lifetime, it is the biggest technical difficulty for the OLEDs because of the limited lifetime of the organic materials.
- High cost at the moment, as the current cost for manufacturing OLEDs is quite high.
- Sunlight effect: the OLEDs display is hard to see in the direct sunlight.
- Sensitive to water, water can easily destroy the organic materials of the displays.
- Low color purity: it is hard for OLEDs display to show very bright and rich colors.

1.1.5 Manufacturing methods of OLEDs

There are three major methods of making OLEDs: vacuum thermal evaporation, spin coating and ink-jet printing.

In the vacuum thermal evaporation process, the material is heated to convert it into vapor in a very short time, and then it is transported to the substrate in a vacuum. There the vapor deposits on the substrate and forms the thin film (Figure 1.4).

In the spin coating process, an excessive amount of a solution is poured on the substrate, and then the substrate is rotated at high speed in order to spread the fluid by centrifugal force. After that, a uniform thin film forms (Figure 1.5).

Ink-jet printing is a procedure of using the piezoelectric inkjet technology to create a pattern by jetting the droplets of the organic ink directly onto substrate (Figure 1.6).

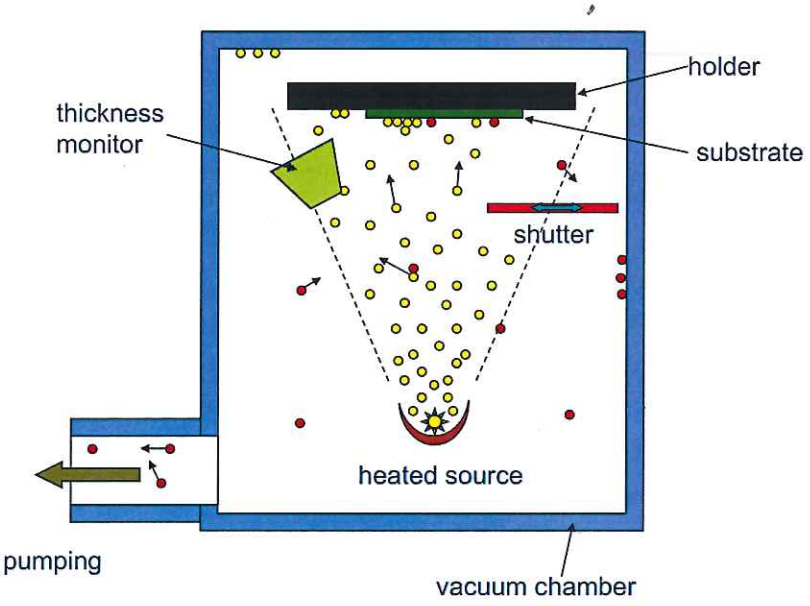

Figure 1.4 Sketch of vacuum thermal evaporation process.

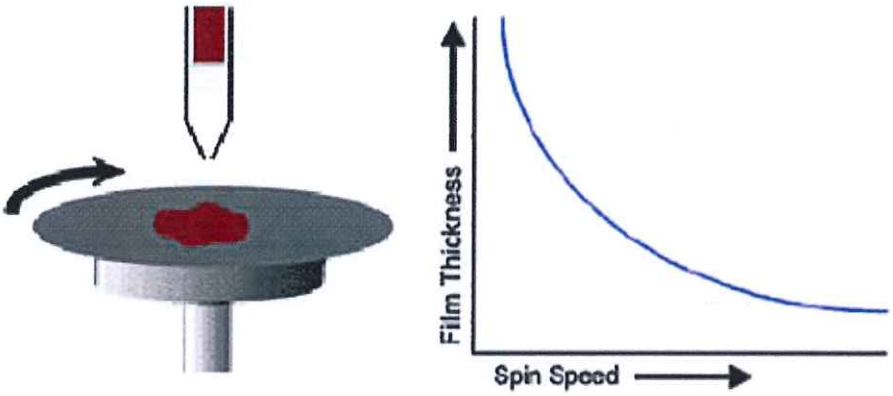

Figure 1.5 Sketch of spin coating process: with an increasing rotating speed, the layer thickness of the film is decreasing [7].

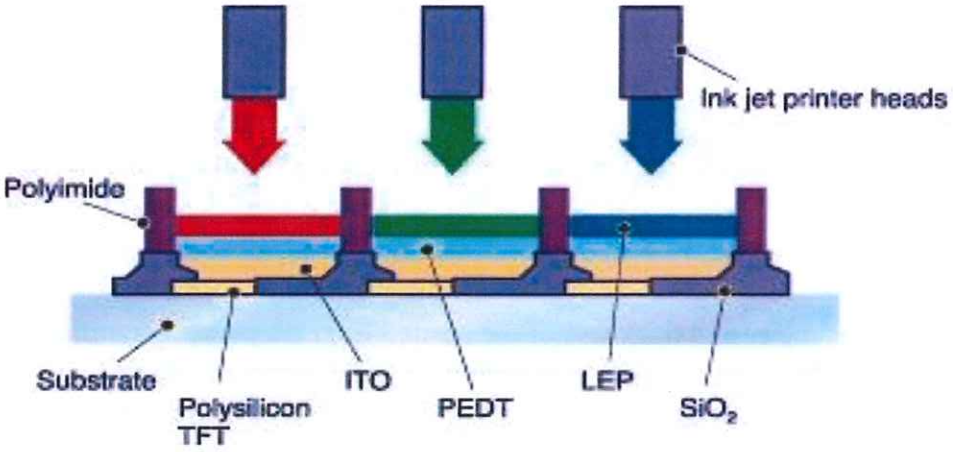

Figure 1.6 Sketch of ink-jet printing processes [8].

Table 1.1 shows the pros and cons of these three manufacturing process of OLEDs:

Manufacturing process	Advantages	Disadvantages
Vacuum thermal evaporation	High purity and homogeneity of the thin film; No substrate damage; High deposition rates; Relatively small substrate heating.	Weak adhesion between film and substrate; Expansive process; Limited use for large area devices.
Spin coating	Easy to operate; Easy to change the layer thickness by changing the spin speed; Easy to get a uniform thin film.	Low material efficiency; Limited use for substrates of different sizes.
Ink-jet printing	High material efficiency; Print on all types substrates with different size; Directly get accurate pattern; Non-contact deposition; Fast process.	Hard to get homogeneous film; Difficulty of jettable ink formulations.

Table 1.1 Pros and cons of three manufacturing processes: Vacuum thermal evaporate; Spin coating and Ink-jet printing

From Table 1.1, it is not hard to find that ink-jet printing has major advantages compared to the other two processes. It is a more efficient way of controlling solution deposition of patterns and delivering small quantities of functional materials locally.

1.2 Problem description

Recently, people have put more and more efforts in the field of ink-jet printing technology improvement. In spite of the basic study of the applications, there are several industrial research challenges that are still outstanding, including the droplet formation and impact of layer formation. All these procedures are influenced by the properties of the ink.

The printability of a material is strongly influenced by molecular weight and concentration. And it is also limited by the viscosity and elasticity of the ink, especially at high molecular weight.

Since the homogeneity and thickness of the printed layer play a very significant role in the OLEDs display performance, it is important to improve the homogeneity of the ink-jet printing films. Unfortunately, after evaporation of a printed film, a ring-like deposit at the edges can be usually observed, which is also called the *coffee stain effect*. This deposit ring affects the homogeneity of the layer, and makes it hard to estimate the layer thickness because the amount of material that has deposited in the ring area is

uncertain. For this purpose, the aim of this work is to optimize the ink formation by the selection of suitable solvent systems and drying strategies of the film after printing, in order to improve the homogeneity of the printed film.

1.3 The scope of the thesis

The overall objective of this thesis is to do the solvent selection and optimization of the drying strategy after ink-jet printing in order to reduce the coffee stain effect and form a uniform layer.

Printed films should have an expected thickness and avoid layer thickness variations. And also the coffee stain at the edge of the films should be reduced. In brief, the newly formulated ink needs to form a homogeneous layer.

The project will concentrate on the solvent selective for the typical organic materials used in OLEDs production and layer formation of these materials. The materials studies in this project are the light emitting polymer (LEP) and the hole injection layer material (HIL).

The thesis contains four major parts:

1. Influence of solvent evaporation rate;
2. Influence of surface tension gradient in the single solvent system;
3. Influence of surface tension gradient in solvent mixtures system;
4. Small molecule OLED devices fabrication with ink-jet printing and performance characterization.

2. Literature review

In this thesis, the main aim is to do the solvent selection and optimization of the drying strategy after ink-jet printing in order to reduce the coffee stain effect and form a uniform layer. In the production of OLEDs by ink-jet printing, the properties of a printed film will influence the properties of the OLEDs. A major difficulty to print a homogeneous layer is the coffee stain generated during the drying procedure.

2.1 Coffee stain effect

2.1.1 Introduction of the coffee stain effect

When a spilled drop of coffee dries on a solid surface, it leaves a dense, ring-like deposit along the perimeter [9], as shown in Figure 2.1. This effect is common when a drop from a solution contains dispersed solute and evaporates on a surface. The ring formation in a sessile drop during the evaporation is a hydrodynamic process. The solids dispersed in the drop are advected to the contact line during the drying process. After all the liquid evaporates, a ring like deposit is left on the substrate that contains most of the solute.

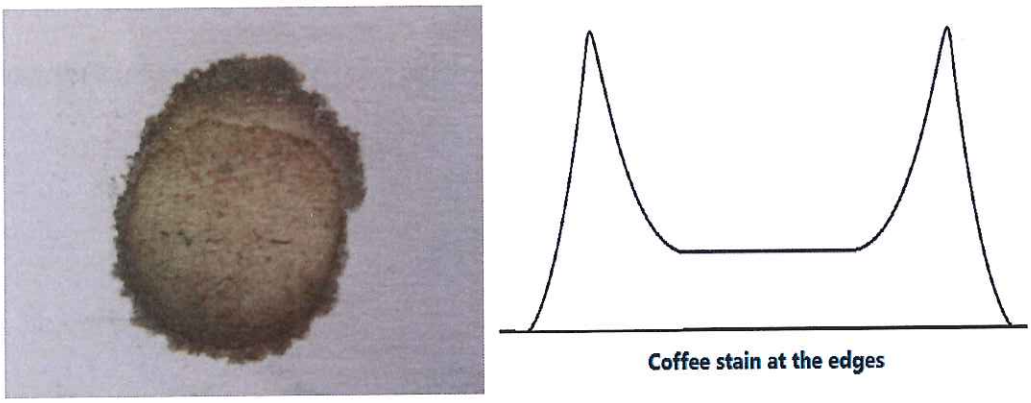

(a) (b)

Figure 2.1 (a) A stain ring of a drop of coffee; (b) Schematic of coffee stain of a printed film.

The ring formation effect impacts the film formation of ink-jet printing and coating processes. After we ink-jet print on a substrate, the solvent of the ink will evaporate into the air, and then the solute will deposit on the substrate. During this procedure, in order to keep the contact line fixed and replenish evaporation losses, liquid is being transported from the center to the edge and forms an outward capillary flow which causes the coffee stain effect [10].

2.1.1 Formation of the coffee stain

Figure 2.2 demonstrates the factors causing outward flow in a small, thin, dilute, circular drop of fixed radius R slowly drying on a solid substrate [9]. As shown in Figure 2.2(a), if there is no contact line pinning, which means no flow, the drop will shrink into the center and deposit there. In order to prevent the shrinkage, and keep the contact line pinning, the solution will have outwards flow, as shown in Figure 2.2(b). While the contact line is pinned, the contact angle is decreased, and during a short time Δt, the region of vertical stripes must be removed from each point r of the surface, as shown in Figure 2.2(c).

The evaporative flux J(r) will control the flow velocity $v_f(r)$, and if the evaporative flux J(r) is available, the flow velocity is known as well. The removed solvent reduces the height h(r) vertically, and the vertically striped region is vacating in a short time Δt. The Figure 2.2(c) has two regions: one is the striped region and the other is the shaded annular region. In the striped region, the volume of this region is equal to the volume removed by evaporation; while in the shaded annular region, the heavy-striped volume is smaller than the volume removed by evaporation (shows in heavy arrows). Thus liquid flows outwards to compensate the lacking volume. In one word, the evaporative rate has strong influence of the coffee stain development.

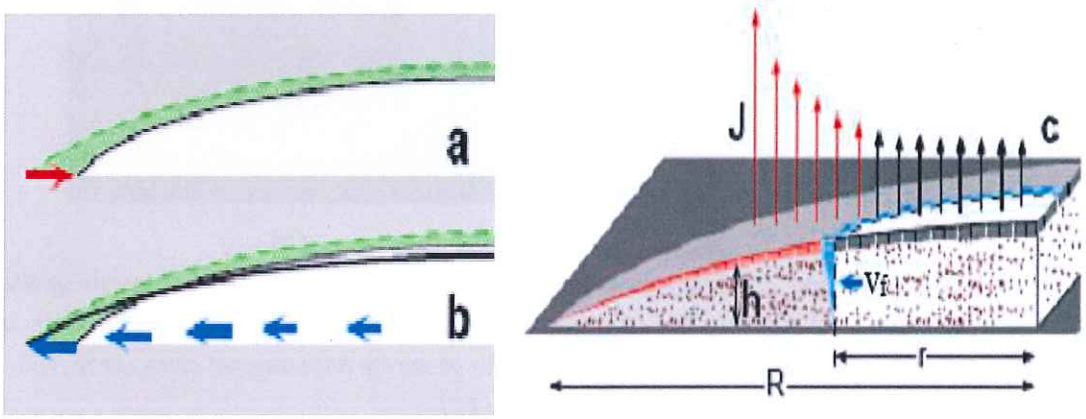

(a) (b)

Figure 2.2 Mechanism of outward flow during evaporation [9]: (a) The evaporation without flow, the droplet shrinks; (b) The replenish flow needs to keep the contact line fixed; (c) The definition of quantities responsible for flow. Vapor leaves at a rate per unit area J(r).

2.2 Marangoni effect

2.2.1 Outline of the Marangoni effect

The Marangoni effect (also called the Gibbs–Marangoni effect) is the mass transfer between two fluids due to surface tension gradient, the molecular transfers from the low surface tension part to the higher part along an interface [11].

The first Marangoni flow considered was the tears of wine phenomenon (Thomson 1885), and the effect is named after Italian physicist Carlo Marangoni, who actually had first published work on the subject 10 years later. The tears of wine phenomenon is readily observed in a glass of the weakest wines following the generation of a thin layer of wine on the walls of the wine glass[12], as shown in Figure 2.3 .

(a) (b)

Figure 2.3 Tears of wine: (a) Seen from the profile, clearly 'tears' in the shadow of this glass of wine with a 13.5% alcohol content[11]; (b) Seen from top, fluid is drawn from the bulk up the thin film adjoining the walls of the glass by Marangoni stresses induced by evaporation of alcohol from the free surface[12].

2.2.1 Principle of the Marangoni effect

If there is a solution with surface tension gradient, because a liquid of a low surface tension pulls much weaker on the surrounding liquid than the one with a high surface tension, so it will cause the liquid to flow towards the regions with high surface tension. Both concentration gradient and temperature gradient can cause the surface tension gradient.

As shown in Figure 2.3, the 'tears of wine' phenomenon is the typical flow due to the Marangoni effect. Since there is a surface tension gradient between alcohol and water,

and the wine is inhomogeneous. The region with a high concentration of alcohol, which means lower surface tension, will be pulled to the region of lower concentration of alcohol, which means greater surface tension [11].

In complex fluids, the morphology of a deposit layer is not only determined by the evaporation and the coffee stain effect, but also the Marangoni effect. For a mixed solution with surface tension gradient, the molecules will transfer from the low surface tension part to the higher part along an interface. So by controlling the surface tension of the compound in the solution, we can form an inward, an outward or a lack of internal flow as shown in Figure 2.4. When the surface tension of the solute is lower than the solvent's, there will be an inward Marangoni flow, while if the surface tension of the solute is higher than the solvent's; there will be an outward Marangoni flow. Thus the Marangoni effect will determine the final shape of the solute deposit [13].

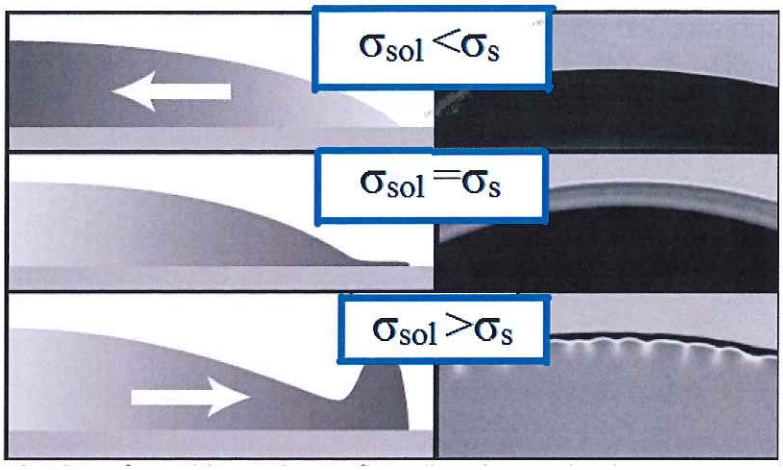

Figure 2.4 A schematic represents the inward, outward and lack of Marangoni flow inside drop, caused by the surface tension gradient of solute and solvent.

2.3 Outline of the thesis

Since the evaporation rate, coffee stain effect as well as the Marangoni effect is all influenced by the temperature, so the appropriate drying temperature and drying method should be chosen.

For ink-jet printing process, before printing, we should first have a good drop formation, according to the different rheological properties of the inks, different printing strategies should also be designed.

Here is the outline of the thesis:

- Drying strategy study and design;
- Single solvent drop formation;
- Single solvent film formation and analysis;
- Solvents mixture influences the film formation;

- Device fabrication and performance characterization.

3. Influence of drying strategies

In this part, we would like to study how to control the coffee stain development by applying different drying strategies. In the project, after the ink-jet printing, a hot plate was used to dry the printed films. We want to optimize the drying temperature and the method to reduce the coffee stain.

3.1 Experiment setup

The experiments are conducted with two drop-on-demand inkjet printers: a Spectra Galaxy and a PixDro LP50. The polymer ink used throughout the experiments is 0.9wt% LEP polymer dissolved in 60% Veratrole + 40% Mesitylene. We print on normal soda-lime glass substrates with a size of 6x6 inch and a thickness of 1.1mm. The glass substrates are cleaned by sequentially applying the following steps: a water spray bath, 5 min in a Teepol solution, 5 min ultrasonic tremble at 60°C in a Deconex solution, 10 min megasoon tremble at 60°C in DI water and 15 min rinses at 60°C in DI water.

We set three different drying conditions for the printed films:

- dry directly on a hot plate;
- dry with a 1mm stainless steel spacer;
- dry with a 1mm stainless steel spacer and a 1mm glass cap(Figure 3.1).

For each case, we use different hot plate temperatures of 50°C, 60°C, 80°C, 100°C, 115°C and 130°C respectively.

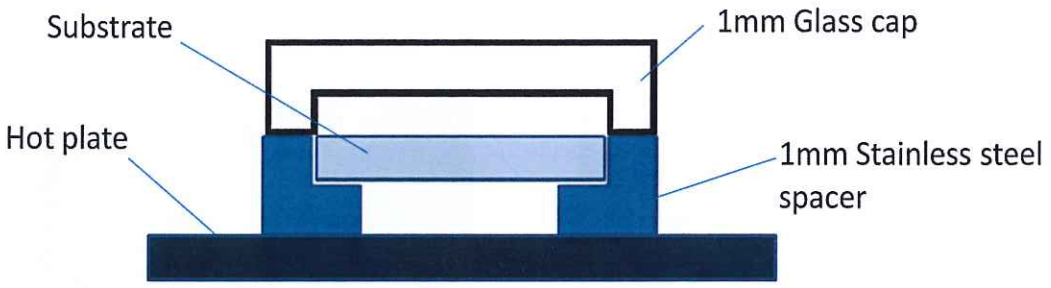

Figure 3.1 Schematic of drying substrate with both spacer and cap.

3.2 Results and discussion

In order to characterize the coffee stain, we first take the microscopy pictures of the dry films, and then scan the surfaces of the films with a Dektak 6M Stylus Surface Profilometer. By scratching several lines at the film center, and scanning with the Dektak, the thickness of the layer can be determined. From the Dektak data, we plot the profile of the printed layers, then define the peak height of the coffee stain as the coffee stain height, the distance from the peak to the edge as the coffee stain width, the

shadow part as the area of coffee stain and the thickness in the center as the layer thickness, all these definitions are shown in Figure 3.2.

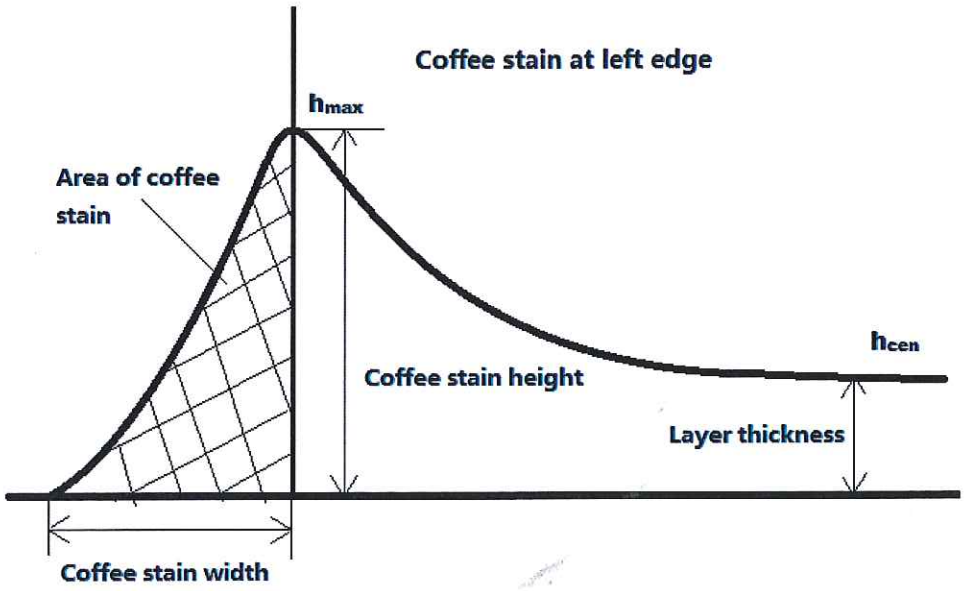

Figure 3.2 Schematic of the definitions for the parameters of a coffee stain: the coffee stain height, the coffee stain width and the coffee stain area.

3.2.1 Drying on a hot plate with/without a spacer

From the microscopy images, films dried with and without a spacer are shown in Figure 3.3. A rectangular ring of deposit material can be observed at the edge, and Figure 3.3 (b) shows a more obvious coffee stain ring compared to Figure 3.3 (a).

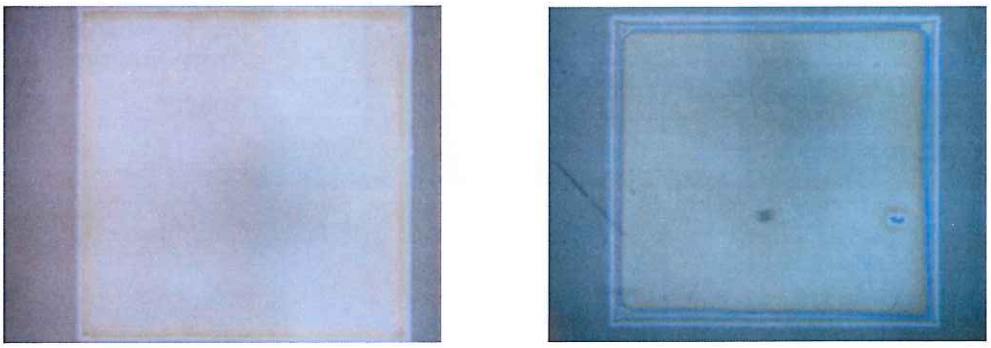

(a) (b)

Figure 3.3 Microscopy images of a 25mm square IJP 0.9wt% LEP polymer in 6V4M on glass, dot pitch: 48μm, line pitch 100μm, dried at 60°C (a) dried with a spacer, (b) dried without a spacer.

Figure 3.4 shows the surface profile scans of the coffee stain part of the films. From Figure 3.4, one can find that when dried without a spacer, the area and height of the

coffee stain on the left and right sides of the film are different: when dried with a spacer the coffee stains at both sides are almost same. Moreover by using a spacer, the height of the coffee stain is decreased quite obviously; as shown in Figure 3.4, the pink and blue lines are the surface profiles of the left and right edges dried without a spacer while the green and yellow lines are dried with a spacer.

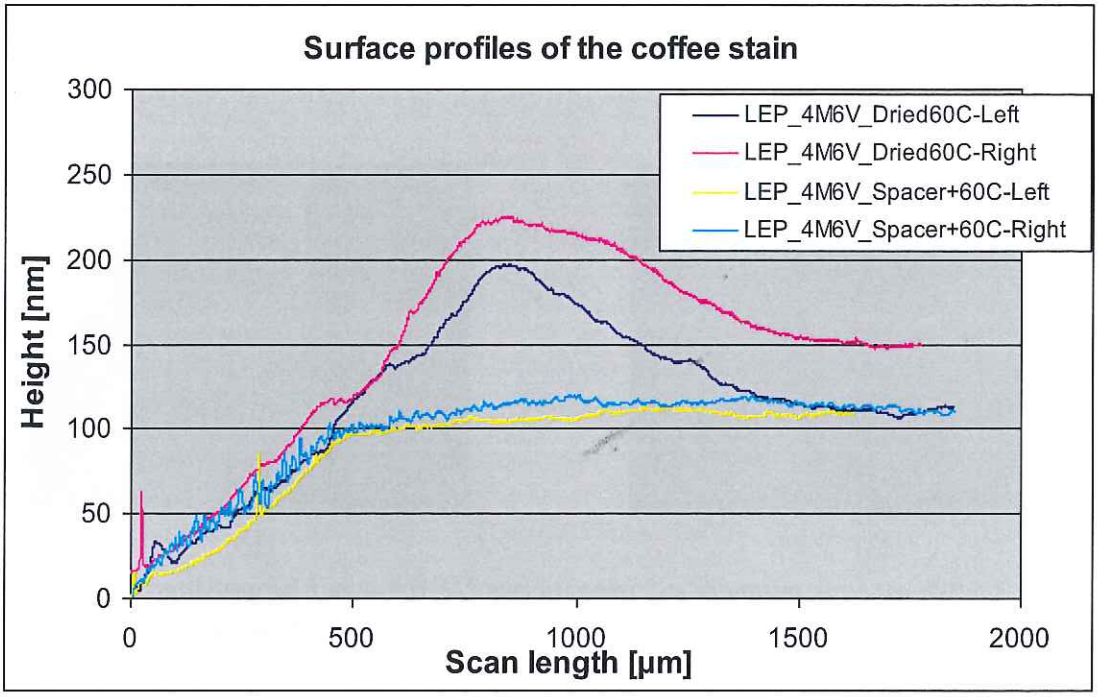

Figure 3.4 Surface profiles of the coffee stain part of 25mm square 0.9wt% IJP LEP polymer in 6V4M on glass, dot pitch: 48µm, line pitch 100µm, dried with and without a spacer at 60°C.

When dried directly on a hot plate, the glass substrate heats up very fast, so the glass substrate deforms and becomes a curved surface. This causes local temperature differences. The temperature variation leads to different evaporation rates along the glass surface, which influences the coffee stain development. This may cause the difference between the coffee stains at left and right edge.

The surface temperature of the glass substrate dried directly on a hot plate is increasing much faster than the one dried with a spacer. Also the stable heating temperature of the substrate will be higher in the first case. The higher temperature leads to higher evaporate rate which cause a stronger capillary force and increase the coffee stain effect.

3.2.2 Drying on a hot plate with a spacer and with/without a cap

Figure 3.5 displays the microscopy images of printed square films with/without a cap: the film in Figure 3.5 (a) is dried only with a spacer, the film in Figure 3.5(b), which has a more serious coffee stain ring, is dried with both spacer and cap. The hot plate temperature is 60°C in both cases.

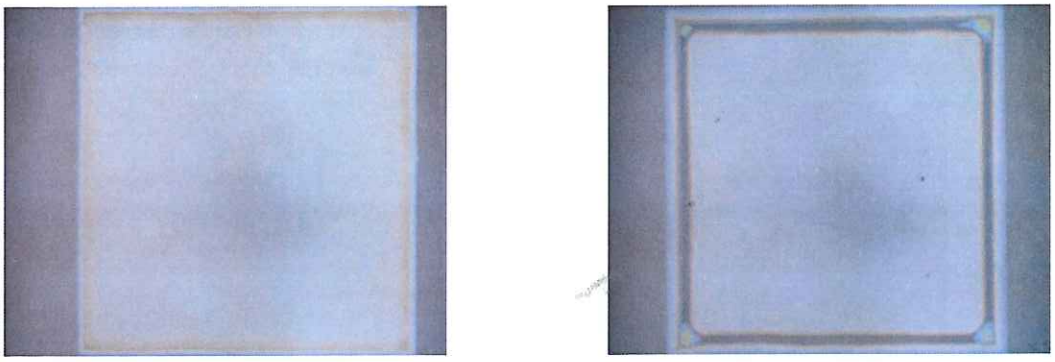

(a) (b)

Figure 3.5 Microscopy image of a 25mm square IJP 0.9wt% LEP polymer in 6V4M on glass, dot pitch: 48μm, line pitch 100μm, dried at 60°C (a) dried with a spacer, (b) dried with a spacer and a cap.

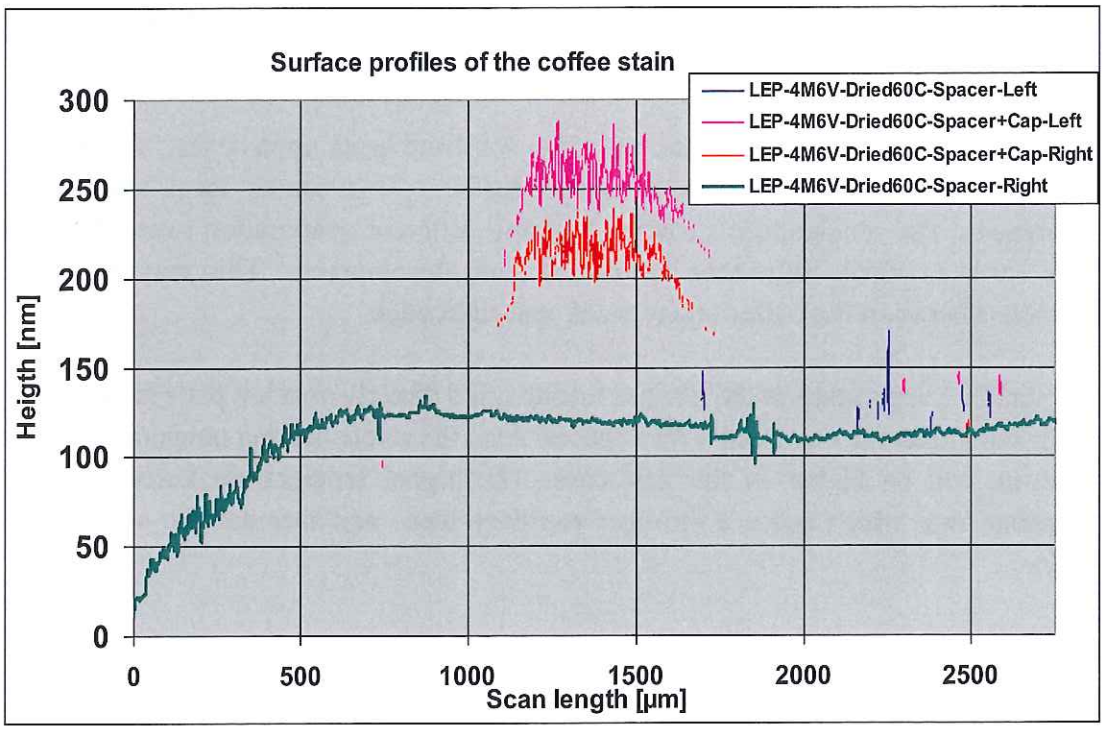

Figure 3.6 Surface profiles of the coffee stain part of 25mm square IJP 0.9wt% LEP polymer in 6V4M on glass, dot pitch: 48μm, line pitch 100μm, one dried with only a spacer, the other one dried with both spacer and cap at 60°C.

In this case, we also used the Dektak to measure the surface profiles. From the graphics of the Dektak data, it appears that drying with a cap and a spacer gives a more serious coffee stain ring as compared to drying only with a spacer. With a cap, the coffee stains are higher and wider, and also tend to go more into the center which leads to a smaller homogeneity area. As shown in Figure 3.6, the pink and red lines are the surface profiles of coffee stain dried with both spacer and cap while the green and blue lines are dried with only a spacer.

When drying with both spacer and cap, the substrate and cap form a relatively closed space, which decreases the drying speed. For the reason, the capillary force affects the coffee stain development for a longer amount of time, causing an increased coffee stain effect.

3.2.3 The relation between coffee stain development and drying temperature, dried with/without a spacer

According to the Dektak data, Figure 3.7 shows the diagrams of the relation between the characterized coffee stain parameters and the drying temperature.

The dependence of the coffee stain on the drying temperature is quite clear: with an increasing drying temperature, the height of the coffee stain is increasing and the width is decreasing. The coffee stain area is relatively constant over temperature. In other words, when increasing the drying temperature, the peak of the coffee stain is increased in height and it moves towards to the edge at the same time. That means the homogenous area of the film becomes larger. And drying with a spacer reduces the coffee stain area by 5X or 6X compared to the situation without spacer.

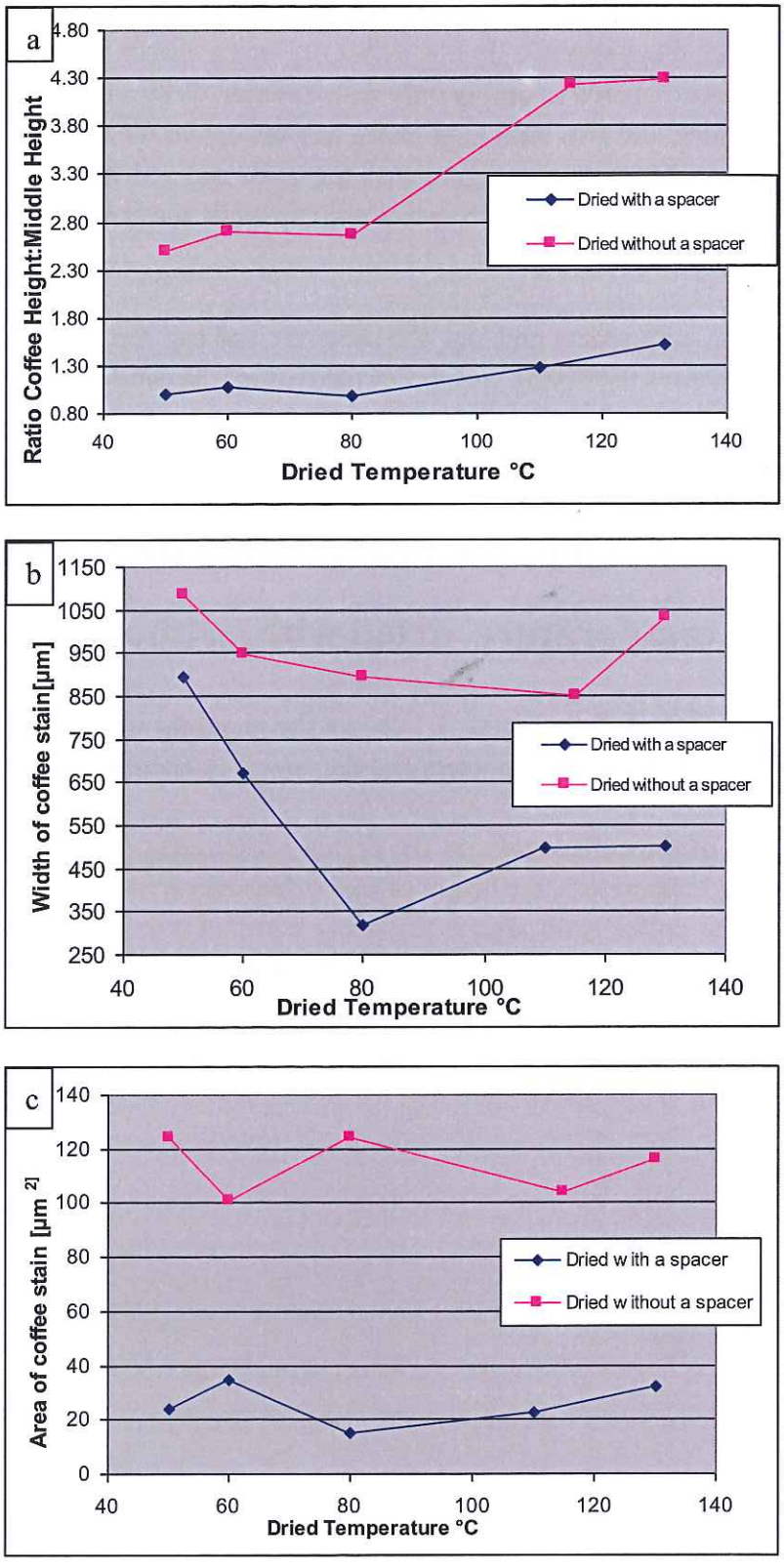

Figure 3.7 Coffee stain characteristics as a function of the drying temperature of 25mm square IJP 0.9wt% LEP polymer in 6V4M on glass, dot pitch: 48µm, line pitch 100µm by LP50, dried with and without a spacer. (a) The ratio of coffee height over middle height; (b) the coffee stain width; (c) the area of the coffee stain.

3.3 Analyses

The evaporation process can be described as follows: when dried on a hot plate, the contact line will pin, and the polymer will deposit, so the evaporation rate at the edge will be faster than at the center. In order to replenish the evaporation losses, the solution is being transported from the center to the edge. Because of this effect, the transportation speed depends on the evaporation rate.

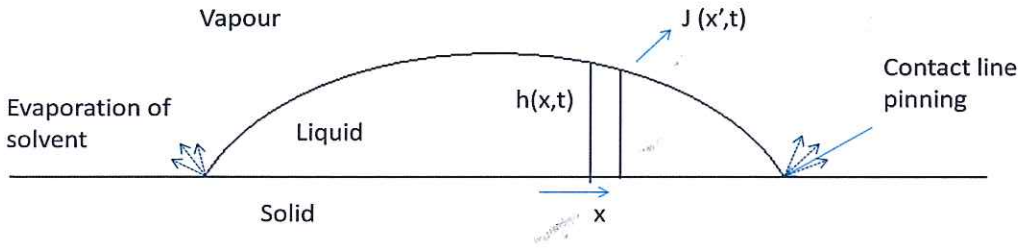

Figure 3.8 Geometry of the evaporation system of a droplet.

We write an equation describing the relationship between the mass flux and heat diffusion during the evaporation process. The state of the system is determined by the height $h(x,t)$ of the cross-section of the droplet as shown in Figure 3.8.

The temperature field $T(x,z)$ satisfies the standard convection-diffusion equation in the liquid which reduces to $\partial^2 T/\partial^2 z=0$ in the long-wavelength approximation [14]. Neglecting density, viscosity, thermal diffusivity and kinetic energy of the gas, the energy balance at the interface gives the heat flux (Oron et al.1997):

$$k\frac{\partial T}{\partial z}\big(z = h(x,t)\big) = -\mathcal{L}_v J \qquad (3.1)$$

$\mathcal{L}_v$ being the evaporation latent heat per unit mass, k the thermal conductivity of the liquid, and J the evaporation rate.

In order to know the temperature changing rate of the substrate surface at different hot plate temperatures when dried with and without a spacer, a thermograph was used to measure the surface temperature of the substrate dried at a certain hot plane temperature. For drying with a spacer, the temperature valve was recorded every 10 seconds in the first minute. For drying without a spacer, it was recorded every 5 seconds in the first 30 seconds. After the initial period, the time spacing of the recording was increased, and the recording was continued until a stable temperature was achieved.

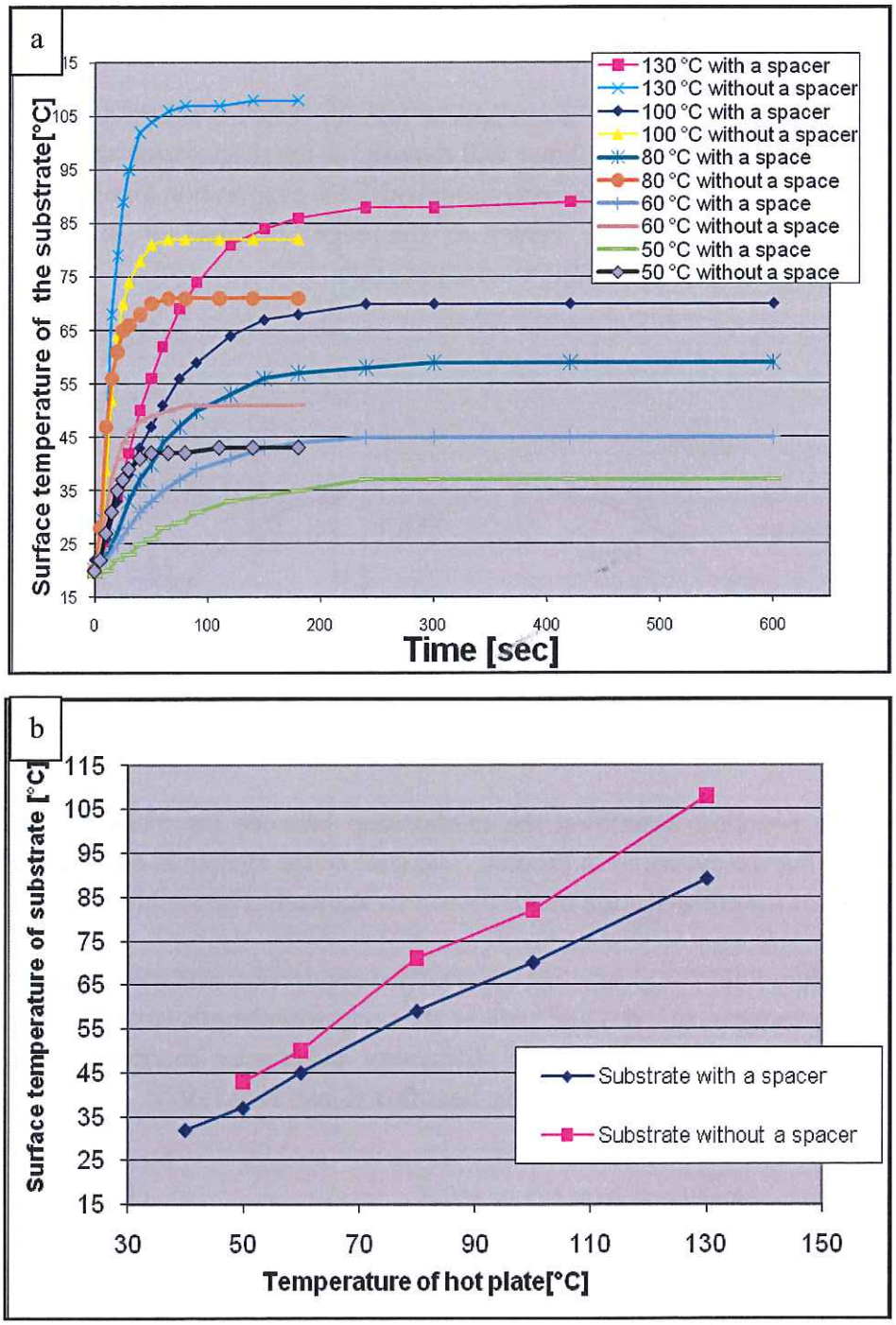

Figure 3.9: (a) The relation between surface temperature and drying time at different temperatures of the hot plane while dried with and without a space; (b) the final stable surface temperature at different temperatures of the hot plane while dried with and without a space

Figure 3.9 (a) shows how the surface temperature changes as a function of time at different hot plane temperatures while the time increased, in both settings of drying with and without a spacer. Figure 3.9 (b) shows the stable substrate surface temperature at different temperatures of the hot plate. From the Figure 3.9, we can easily find that the temperature changing rate when dried the substrate without a spacer is much faster

than the rate of dried with a spacer. From equation 3.1 we know that when the temperature changing rate increases, the evaporation rate J will increase too. This makes the coffee stain effect worse, and leads to a higher coffee stain.

3.4 Summary

In this part, it is found that drying only with a spacer can considerably reduced the height and the width of the coffee stain, compared to the cases that dry without a spacer and with both spacer and cap. The ratio of coffee height over middle height when drying with a spacer is almost 1/3 of the case when drying without a spacer. However, the width of the coffee stain is reduced 1/2 when drying with a spacer. At the same time, the difference between the coffee stains at the left and right sides also decreased when dried with a spacer.

With an increasing drying temperature, the height of the coffee stain is increasing while the width is decreasing. Thus the area of the coffee stain does not change with the changing temperature. The optimal drying strategy is drying at 80°C with a spacer, because the ratio of coffee height over middle height, the width and the area of the coffee stain are at the minimum values. For some material which cannot stand high drying temperature, we also can dry at 60 °C, which also reduce the coffee stain to a certain level.

4. The influence of the surface tension gradient of single solvent systems

The previous chapter studied the control of the coffee stain development by choosing different drying strategies which affect the evaporation rate. Apart from the evaporation rate, the Marangoni effect also impacts the surface coffee stain of the printed layers, and will be studied in this chapter. In order to get more reliable results we will use three different types of material in this part. The first two materials are LEP materials including white LEP and blue LEP and the other one is the HIL material: they are all widely used in the production of OLED devices.

Because the Marangoni effect is caused by the surface tension gradient along the interface, we would like to choose a set of solvents with a variety of surface tensions compare to the surface energy of the solute materials.

4.1 The study of white LEP material

4.1.1 Experiments setup

We first measure the surface energy of the white LEP by spin-coating a white LEP substrate, and then characterizing the surface energy using the KRÜSS Easy Drop standard. The obtained surface energy of the white LEP is 31 mN/m.

According to this value, we screen the solvents in which the white LEP material can dissolve, leading to the four solvents shown in Table 4.1. As can be seen, these solvents have a variety of surface tensions:

Solvent	Boiling point (°C)	Density (20°C) g/ml	Viscosity (20°C)mPa.s	Surface tension (20°C)mN/m
Mesitylene	166	0.865	0.70	27.8
Phenetole	168	0.965	1.23	31.4
Indane	176	0.960	1.40	32.6
Veratrole	207	1.084	3.64	39.3

Table 4.1 Selected solvents list for the white LEP material and measured properties.

For this work, we prepare the inks with the white LEP polymer, dissolved in the pure solvents of Mesitylene; Phenetole; Indane; Veratrole separately. Since it is found that the solution of the LEP polymer in Veratrole becomes a gel at room temperature it cannot be used for testing.

For the other three inks, we measure the viscosity, density and surface tension of those inks. The equipments we use are the AMVn Automated Microviscometer and the KRÜSS Easy Drop standard. Table 4.2 shows the characterized properties of the inks.

Solution (0.9wt %)	Density (20°C) g/ml	Viscosity (20°C)mPa.s	Surface tension (20°C)mN/m
W-LEP in Indane	0.961	10.02	32.9
W-LEP in Phenetole	0.966	7.97	30.06
W-LEP in Mesitylene	0.868	2.18	27.81

Table 4.2 The physical properties of the white LEP inks

After characterizing the properties of the inks, we use two methods to study the coffee stain development for the solvents with different surface tension gradients:

- Wetting
  Use the Easy Drop to form a certain volume droplet wetting on a small glass substrate (30mmx30mm) for each ink. Then first dry it on a 60°C hot plane, then annealing it at 180°C.
- Ink-jet Printing with Dimatix
  Besides the wetting experiments, we also do the ink-jet printing with the Dimatix Materials Printer. For each ink, we print 25x25 mm squares on glass or spin coated Pedot:PSS substrates at various DP. Then dry at 60°C with a 1mm spacer on a hot plane, and annealing it at 180°C.

After preparing all the samples, microscopy photos are taken first to see the morphology of the layer, then the Dektak is used to determine the surface profile and thickness of the dried layer.

4.1.2 Results and discussion

4.1.2.1 Droplet wetting on a glass substrate by Easy Drop

Figure 4.1 shows the microscopy images and the surface profiles of the dried droplets, from these pictures you can find that in Figure 4.1(a), most of the polymer have deposited in the center, droplet in Figure 4.1(b) has a more uniform layer, while in Figure 4.1(c) the homogeneity of the dried layer is really bad, much stronger coffee stain effect can be observed in this case.

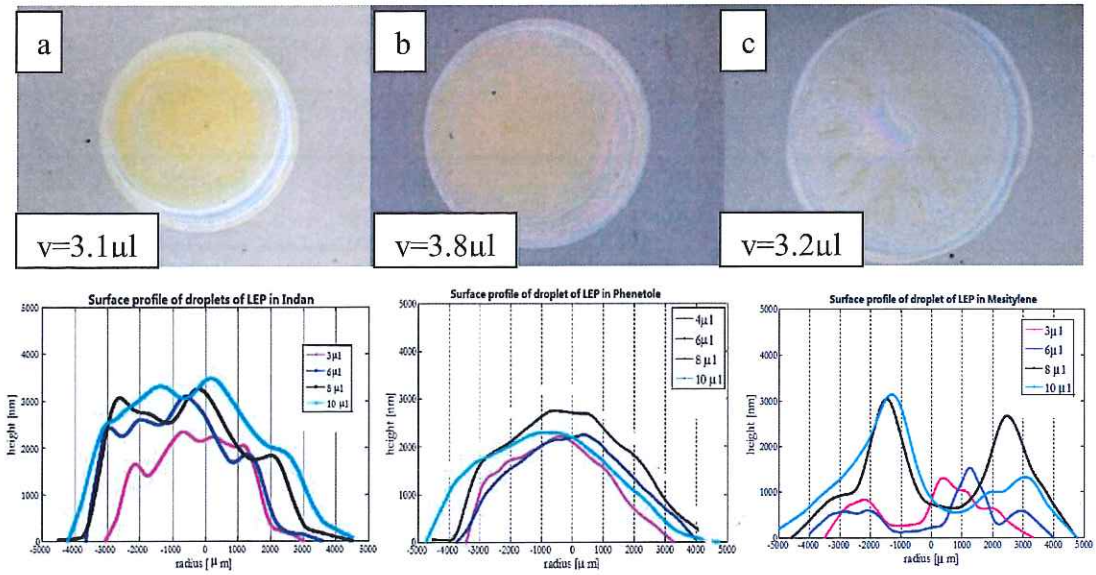

a. $\sigma_p - \sigma_s = -1.6$ b. $\sigma_p - \sigma_s \rightarrow 0$ c. $\sigma_p - \sigma_s = +3.4$

Figure 4.1 Final morphologies and surface profiles of the polymer deposit of different surface tension gradients on glass substrates by Easy drop. In profile 1(c), the coffee stain is very obviously.

From these results, we can observe that the volumes of the droplets will not influence the coffee stain development. On the other hand, the three solution result in different coffee stains, due to the variation of the surface tension gradient of the polymer and solvent.

4.1.2.2 Ink-jet Printing with Dimatix

Figure 4.2 and 4.3 are the microscopy images of the printed squares with the inks which have surface tension gradients between the polymer and solvent.

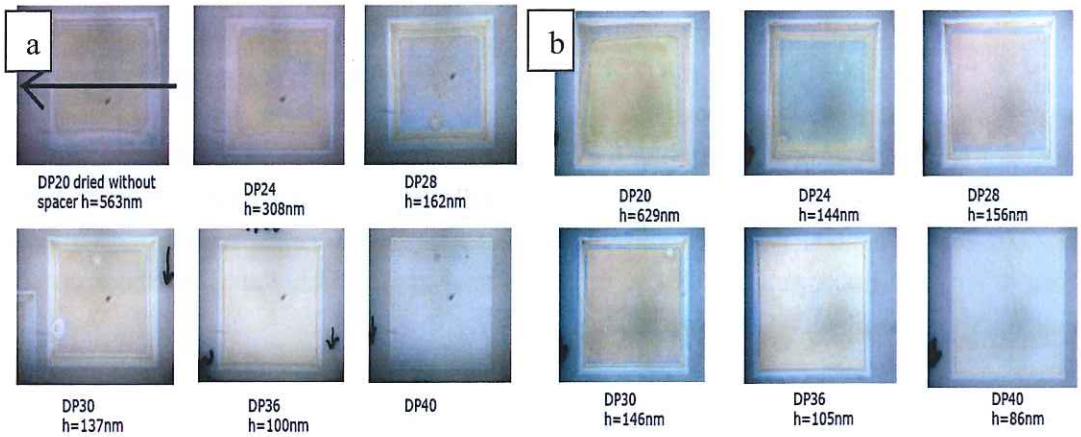

Figure 4.2 Final morphologies of IJP 0.9wt% white LEP in Indane ($\sigma_p - \sigma_s = -1.6$) with different DP and the measured layer thickness in the center: (a): IJP on glass substrate, when DP is 40, no homogeneous layer is formed, so measure the thickness in the center cannot be measured; (b): IJP on spin coated Pedot: PSS substrate.

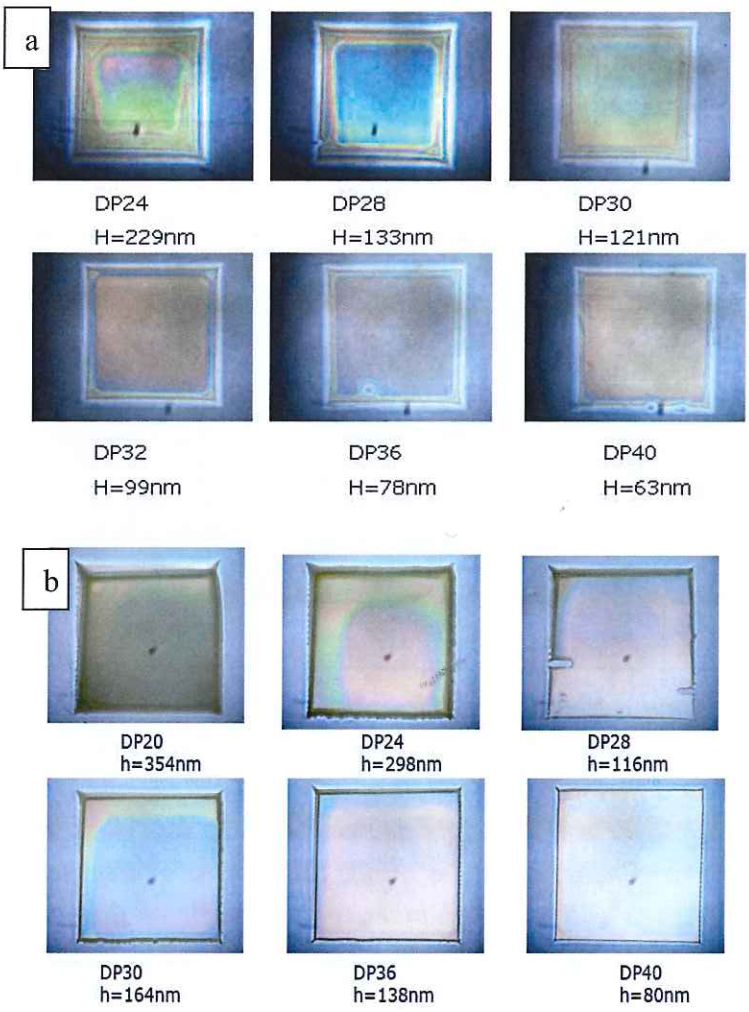

Figure 4.3 Final morphologies of IJP 0.9wt% white LEP inks with different DP on spin coated Pedot: PSS substrate and the measured layer thickness in the center: (a) white LEP in Phenetole (σ_p- $\sigma_s \rightarrow 0$); (b) white LEP in Mesitylene (σ_p- σ_s= +3.4).

With the experimental results in Figure 4.2, we find that for IJP of white LEP ink, there is no difference between printing on glass and Pedot. The only difference is that the wetting of the ink on Pedot is better than on glass, so we can print thinner layers on Pedot substrate with a higher DP.

Next, the Dektak is used to characterize the surface coffee stain and the layer thickness. The coffee stain effect is estimated from the average ratio of the coffee stain height and the height in the middle of the printed area with different DP for these inks as discussed in chapter 3. The definition of all the parameters can be found in Figure 3.2 in chapter 3. The entire scan of the Dektak is from right to left like the arrow shown in Figure 4.2(a). With those data we plot the graphics of the relation between the DP and the coffee stain development with different surface tension gradients, as shown in Figure 4.4.

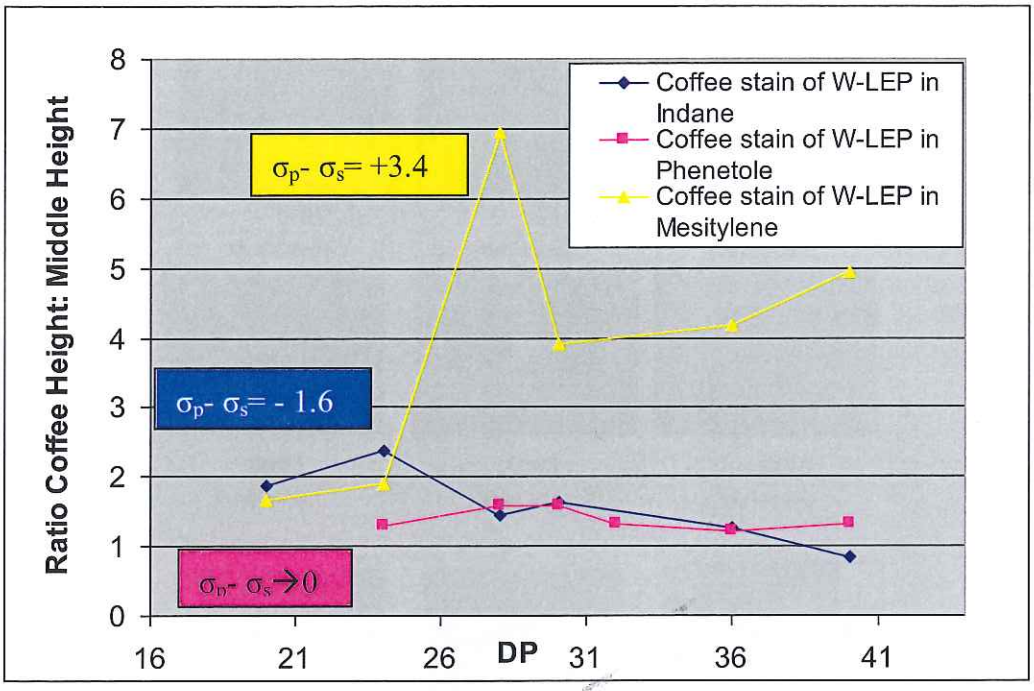

Figure 4.4 Coffee stain estimation as a function of printing dot pitch of 25mm square IJP 0.9wt% white LEP inks of different surface tension gradient between polymer and solvent on spin coated Pedot:PSS. For IJP of 0.9wt% LEP in Indane (σ_p- σ_s=-1.6), the ratio of coffee height over middle height decreased while the DP increased; for IJP of 0.9wt% white LEP in Phenetole (σ_p- σ_s →0), the ratio of coffee height over middle height does not change with the DP increased; for IJP of 0.9wt% white LEP in Mesitylene (σ_p- σ_s= +3.4), the ratio of coffee height over middle height increased while the DP increased.

From Figure 4.4, it is clear that inks with different surface tension gradients between polymer and solvent have different trends of the coffee stain development with increasing DP. The blue line is the surface coffee stain of IJP 0.9wt% white LEP in Indane (σ_p- σ_s=-1.6). In this case, there is an inwards Marangoni flow during drying, so the coffee stain is reduced. For increasing DP, the printed layer will be thinner. With a thinner layer, due to the shorter evaporation time, the Marangoni effect plays the dominant role in the formation of the coffee stain. Since the Marangoni flow is inwards, the coffee stain is further reduced.

However, the yellow line is the surface coffee stain of IJP 0.9wt% white LEP in Mesitylene (σ_p- σ_s= +3.4) which behaves in a totally opposite way. In this case, there is an outwards Marangoni flow during drying, leading to a higher but much narrower coffee stain at the edges. Now, the effect of the Marangoni flow is stronger when the printed layer is thinner. The pink line shows the surface coffee stain of IJP 0.9wt% white LEP in Phenetole (σ_p- σ_s → 0). In this case, only the capillary force caused by the different evaporation rates at the edge and center of the film affects the coffee stain development. So this line is almost constant with the DP increasing.

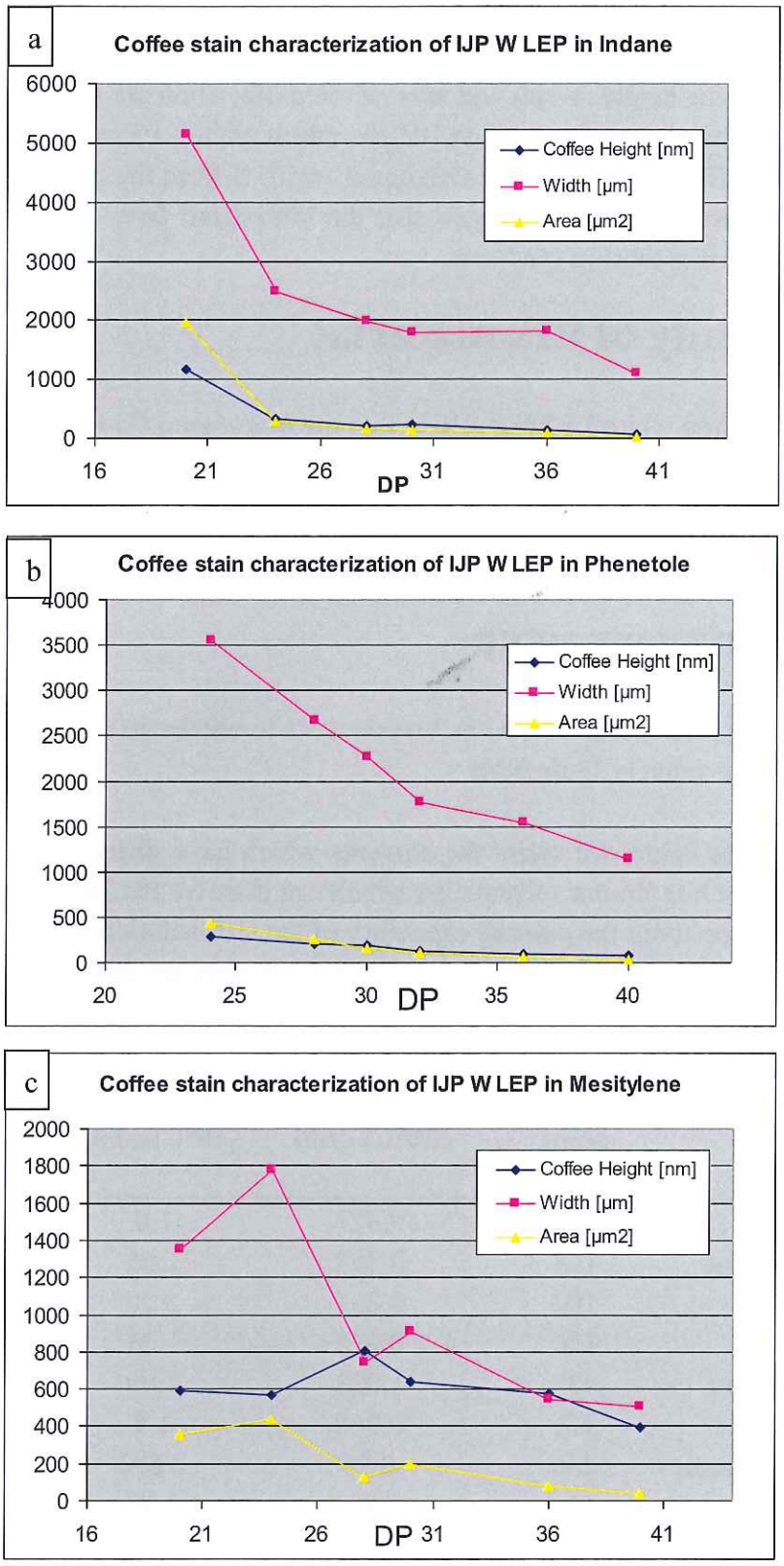

Figure 4.5 Coffee stain characteristics change with the DP variation of IJP LEP in different solvents on spin coated Pedot:PSS substrate, we characterize the height, the width and the area of the coffee stain: (a) 0.9wt% white LEP in Indane (σ_p- σ_s=-1.6) ; (b) 0.9wt% white LEP in Phenetole (σ_p- $\sigma_s \rightarrow 0$); (c) 0.9wt% white LEP in Mesitylene (σ_p- σ_s = +3.4).

Figure 4.5 shows the changing of the height, width and area of the coffee stain with a decreasing layer thickness of IJP with different white LEP inks. It is clear that for all these three inks, the height, width and area of the coffee stain are decreasing with the layer thickness decreasing. For a given DP, the ink of white LEP in Mesitylene results in the highest coffee stain, while the maximum width is from the ink of white LEP in Indane. The measurements also suggest that the Marangoni flow is different for inks with different surface tension gradients.

4.2 The study of HIL material

The results from the white LEP inks show that the Marangoni flow does influence the coffee stain development. In order to see whether the theory works with different types of material or not, we choose the HIL material to do similar experiments to verify the results.

4.2.1 Experiments setup

We use the same method mentioned in Section 4.1.1 to obtain the surface energy of the HIL material, the value is 33.6mN/m.

According to this value, we select the solvents which have different surface tension compare to the solute from a solvents list which can dissolve the HIL material. Due to lack of experience about the pinning capability of the HIL solution for ink-jet printing, a larger amount of solvents is used for testing: ten solvents are selected and are shown in Table 4.3.

Solvent	Boiling point (°C)	Density (20°C) g/ml	Viscosity (20°C)mPa.s	Surface tension (20°C)mN/m
p-cymene	178	0.877	1.0	27.49
n-Butylbenzene	183	0.863	1.06	27.81
Decalin	192	0.881	2.50	30.11
Phenetole	170	0.965	1.23	31.44
Propylbenzoate	231	1.023	2.69	32.43
Indane	176	0.960	1.4	32.6
Cyclohexylbenzene	240	0.95	2.863	33.56
Anisole	154	0.994	1.07	34.03
Tetralin	207	0.969	2.18	34.33
Methylbenzoate	200	1.088	2.05	35.97

Table 4.3 Selected solvents list for the HIL material and measured properties.

Then, the HIL inks are prepared from the selected ten solvents and the physical properties of those inks are characterized, as shown in Table 4.4.

Solution (5mg/ml)	Density (20°C) g/ml	Viscosity (20°C)mPa.s	Surface tension (20°C)mN/m
HIL in p-cymene	0.877	2.92	27
HIL in n-Butylbenzene	0.864	2.95	27.87
HIL in Decalin	0.882	7.59	29.66
HIL in Phenetole	0.964	3.64	31.41
HIL in Propylbenzoate	1.02	7.84	32.36
HIL in Indane	0.960	4.37	32.96
HIL in Cyclohexylbenzene	0.944	8.87	32.48
HIL in Anisole	0.994	2.83	33.63
HIL in Tetralin	0.969	6.97	34.62
HIL in Methylbenzoate	1.09	5.71	35.44

Table 4.4 The physical properties of the HIL inks

With all these HIL inks, we do the ink-jet printing test with the Dimatix Materials Printer. For each ink, we print 20x20 mm squares on spin coated Pedot: PSS substrates at various DP. Then the samples are dried at 80°C with a 1mm spacer on a hot plane, and then annealed at 180°C.

After finishing preparation of all the samples, microscopy photos are taken first to see the morphology of the layer, then the Dektak is used to obtain the surface profile and thickness of the dried layer.

4.2.2 Results and discussion

After ink-jet printing tests, we observe that most of the inks cannot form homogeneous layers. Some of them do not have the contact line pinning at the edges, and most of the material shrinks into a small area during the drying process and deposits there. Some of them retract into very small single drops and pin locally, instead of merging together and forming a uniform layer. Only two inks: HIL in n-Butylbenzene and HIL in Decalin, have good layer formation after ink-jet printing with the Dimatix printer.

Figure 4.6 shows the morphologies of the dried layers under UV light by ink-jet printing with the eight inks that do not have good pinning at the edges and no formation of a homogeneous layer.

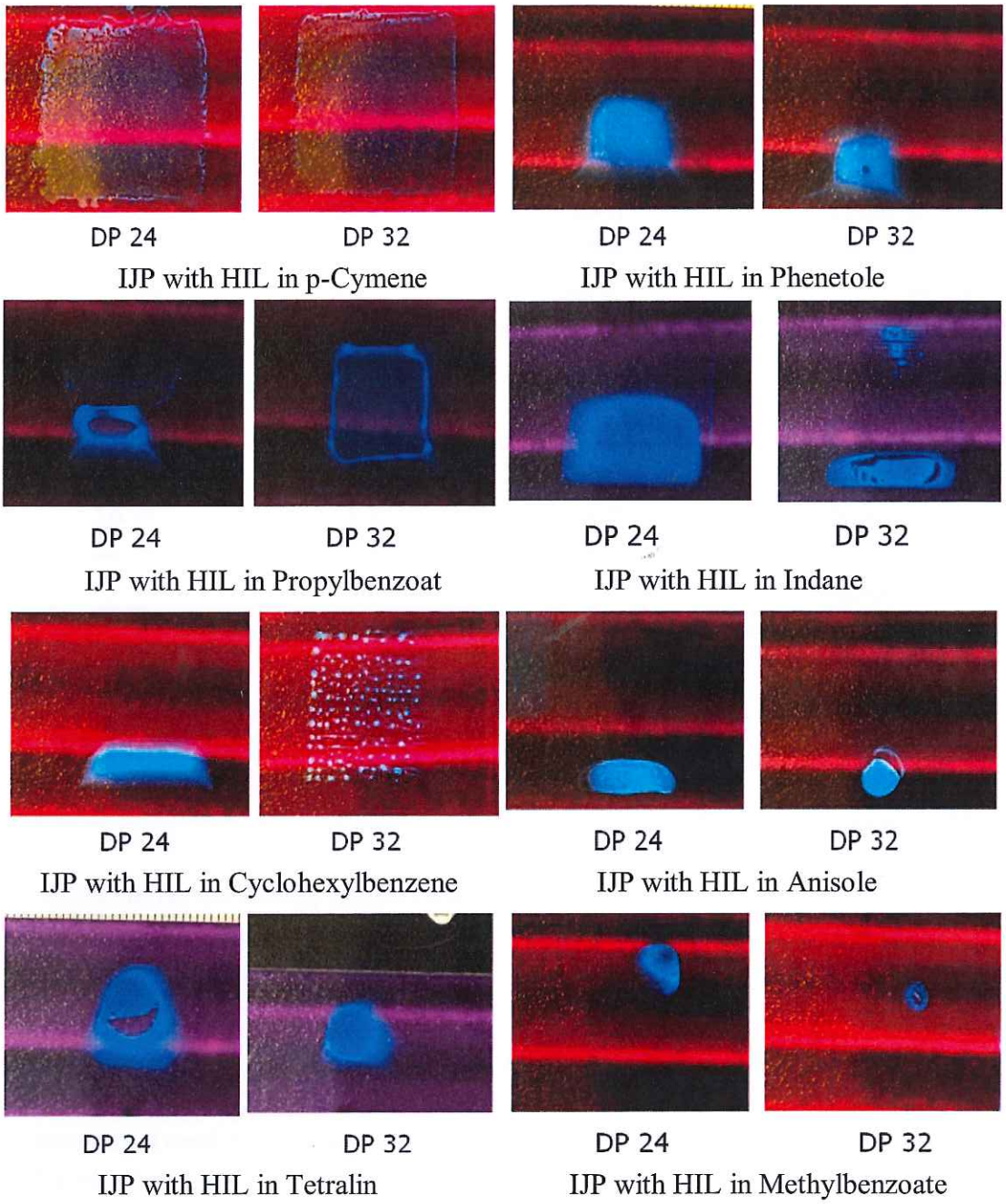

Figure 4.6 Final morphologies of the dried layers under UV light by IJP with the inks of HIL material in different solvents. All kinds of problems are found here: no contact line pining and dewetting.

In order to have pinning, the contact angle between the droplet and the substrate cannot be zero. If the contact angle is zero, no pinning occurs, and the drop will spread unlimited. In our cases, the contact angle is always above zero. There are two modes during drying of a droplet [15], as shown in Figure 4.7.

1. Constant contact angle and decreasing contact area;
2. Decreasing contact angle and constant contact area.

Contact line pinning occurs at the second situation.

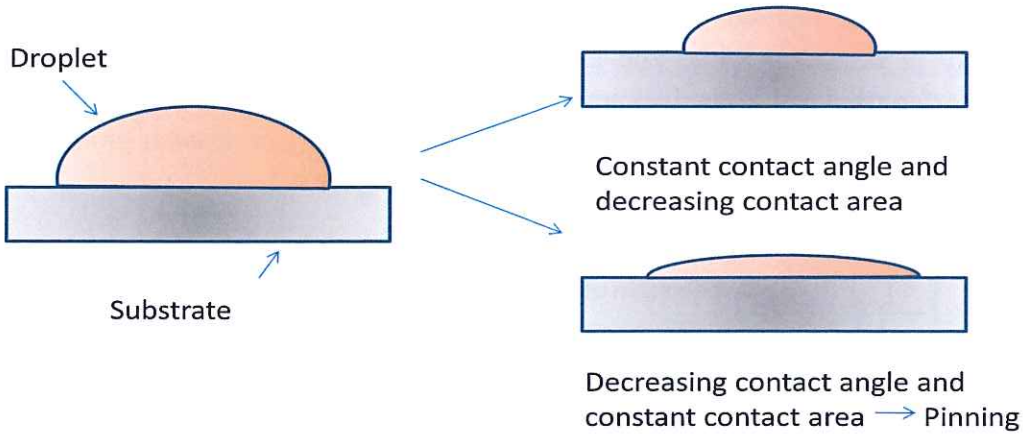

Figure 4.7 Two modes during drying of droplet: constant contact angle and constant contact area.

In the case of contact line pinning, the contact angle retracts while the surface area exposed to the substrate remains constant. To maintain contact line pinning while the mass is reduced during the evaporation process, the sum of the adhesive force between the dispersed solute and the substrate must stronger than the solvent and substrate interaction.

The above is the general idea about the pinning effect. During the study, we also found another phenomenon: an ink which can pin with ink-jet printing with the Galaxy printer and LP50 printer may not work with Dimatix printer. This will be further discussed in chapter 5. What the decisive factors are to control the pinning and how to predict if a solution will pin or not still needs more research.

As opposed to the inks shown in the previous figure, the inks of HIL in n-Butylbenzene and HIL in Decalin form homogeneous films after ink-jet printing with the Dimatix printer, as shown in Figure 4.8.

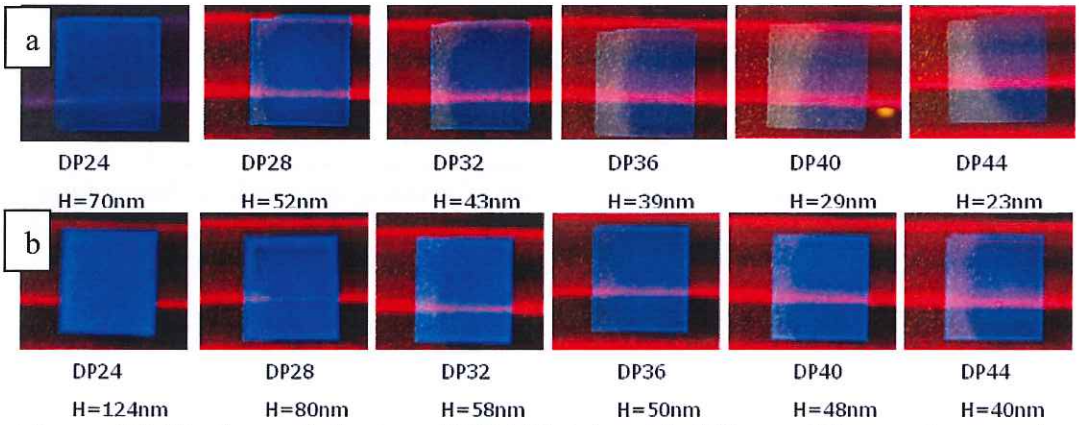

Figure 4.8 Final morphologies of IJP HIL inks with different DP on spin coated Pedot: PSS substrate under UV light and the measured layer thickness in the center: (a) HIL in n-Butylbenzene (σ_{HIL}- σ_s= +5.8); (b) HIL in Decalin (σ_{HIL}- σ_s= +3.5).

We use the same method to estimate the coffee stain development as mentioned previously in section 4.1.1.2. The Dektak profilometer is used to characterize the surface coffee stain and layer thickness. Then, the graphics of the relation between the DP and the coffee stain characterizations with different surface tension gradients are generated with this data, as shown in Figure 4.9 and Figure 4.1.

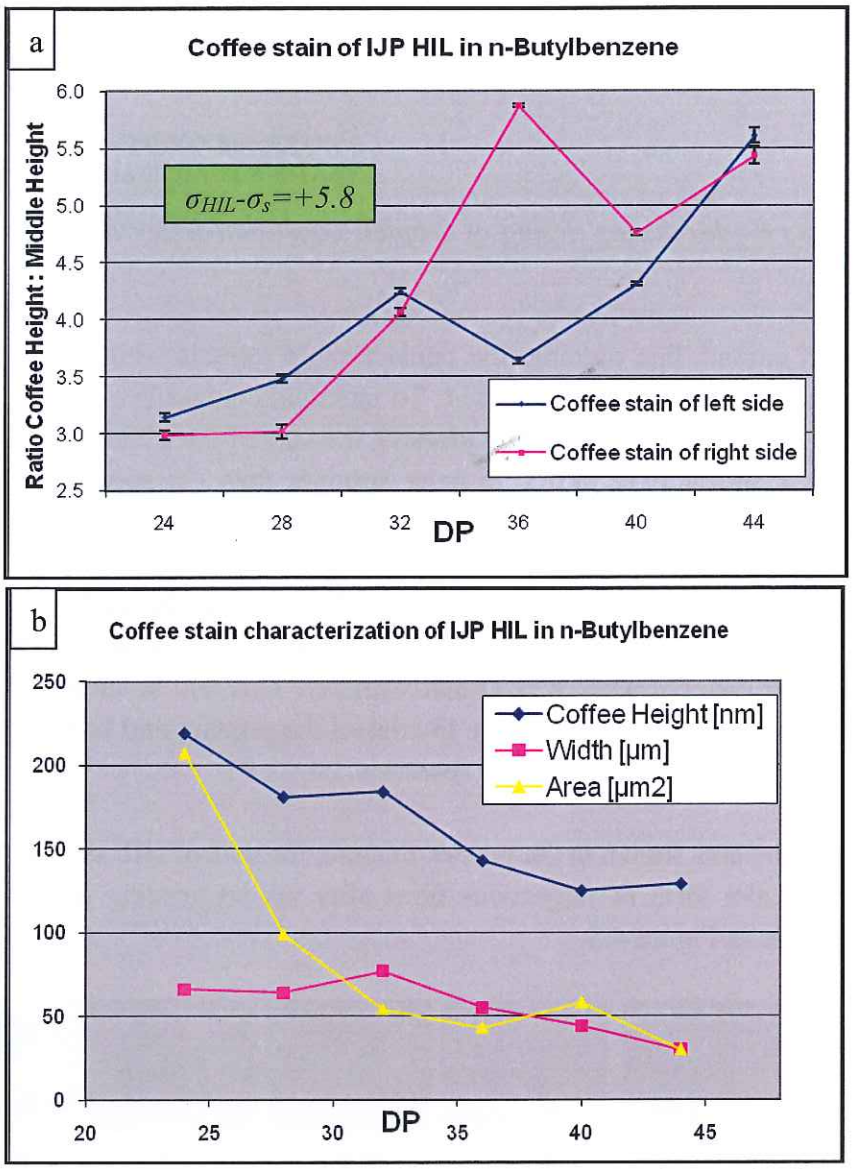

Figure 4.9 Coffee stain estimation as a function of printing dot pitch of 20mm square IJP ink of HIL in n-Butylbenzene (σ_{HIL}- σ_s= +5.8) on spin coated Pedot:PSS: (a) the ratio of coffee height over middle height increases while the DP increases;(b) the height, width and area of the coffee stain decease while the DP increases.

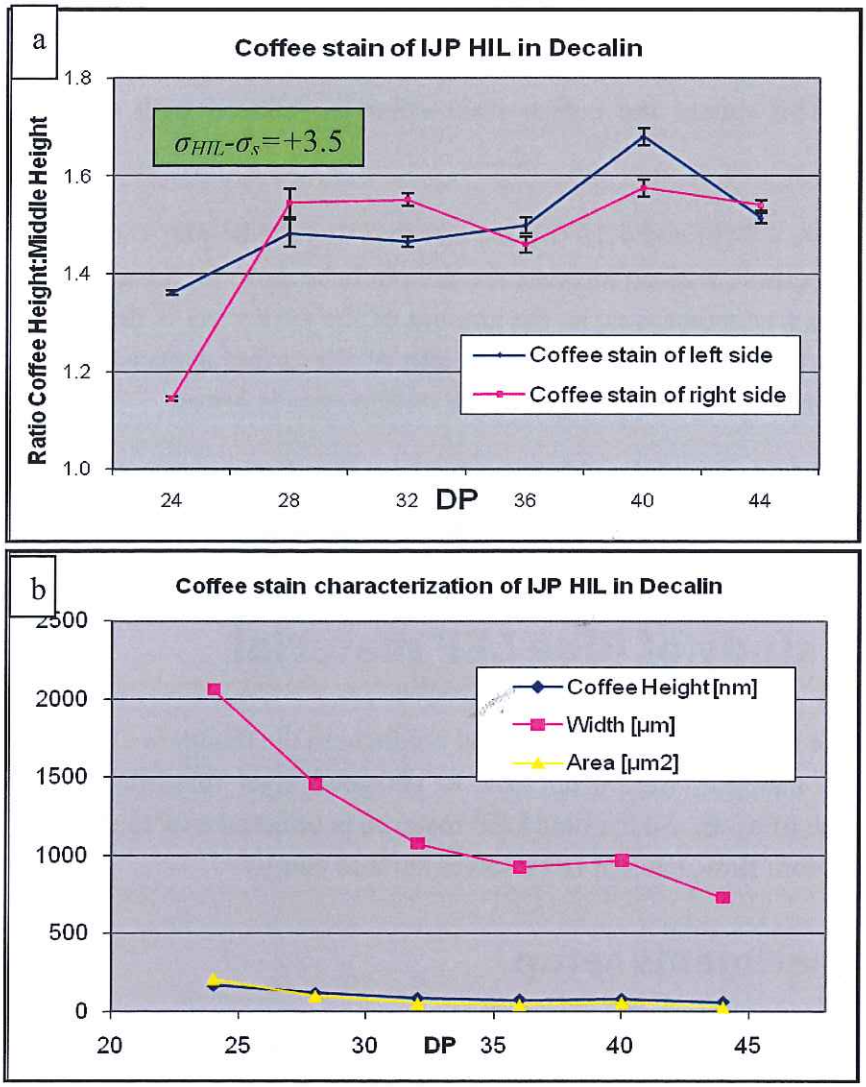

Figure 4.10 Coffee stain estimation as a function of printing dot pitch of 20mm square IJP ink of HIL in Decalin (σ_{HIL}- σ_s= +3.5) on spin coated Pedot:PSS: (a) the ratio of coffee height over middle height increases while the DP increases, but the slope of the line is relatively small;(b) the height, width and area of the coffee stain decease while the DP increases.

Figure 4.9 (a) and 4.10 (a) shows how the surface coffee stain changes as a function of dot pitch. It is clear that for both inks, the ratio of coffee height over middle height increases with the DP increases, because the surface tension of these two solvents are lower than the surface energy of the HIL material, and cause an outwards Marangoni flow. With a thinner layer, due to the shorter evaporation time, the Marangoni effect plays the major role in the coffee stain formation, so the slope of the trend line is positive in both cases.

Since the distinction of the surface energy of HIL and the surface tension of Decalin is much smaller than for the other ink (HIL in n-Butylbenzene), so the Marangoni effect is much weaker for the ink of HIL in Decalin, which is demonstrated by a reduced slope in Figure 4.10(a), as compared to Figure 4.9(a).

Comparing the values of the ratio between coffee height and middle height of a same dot pitch of these two inks, it is shown that a solvent with a higher surface tension has a lower ratio. This means the coffee stain effect is reduced with increasing surface tension.

While in Figure 4.9 (b) and 4.10 (b), we can find that the height, width and area of the coffee stain decrease with an increase the dot pitch, because for a higher DP means less droplets jets at a constant area, so the amount of the jetting ink is decreasing to form a thinner layer. It is also shown that the width of the coffee stain is wider in a higher surface tension ink, while the height of the coffee stain is lower.

All the results from the HIL inks show same influence of the Marangoni flow in the coffee stain development like white LEP inks. It means the theory also works with HIL material.

4.3 The study of Blue LEP material

Until now, the results are as expected, and conform to the theory in chapter 2. But in the study of HIL material, we are not able to get good layer formation in the case of a negative value of σ_p- σ_s. So the blue LEP material is selected now to study the influence of the Marangoni flow, since it has a lower surface energy

4.3.1 Experiments setup

The accurate value of the surface energy of the blue LEP material is measured by the KRÜSS Easy Drop standard, and the value is 27.7 mN/m.

In this part, we want to study the coffee stain development in case of a solvent with a higher surface tension than the solute. So we select a solvent which surface tension is larger than 27.7 mN/m from the solvents list which can dissolve the blue LEP material.

Thus, Phenetole is selected as the solvent which has a higher surface tension. In order to have some comparable results, we also choose two more solvents: Mesitylene and 3-Methylthiophene. We make the blue LEP ink using these three solvents and characterize the properties of the inks, as shown in Table 4.5.

Solution (0.9wt %)	**Density (20°C) g/ml**	**Viscosity (20°C)mPa.s**	**Surface tension (20°C)mN/m**
B-LEP in Phenetole	0.965	5.94	30.45
B-LEP in 3-Methythiophene	1.02	2.5	27.35
B-LEP in Mesitylene	0.868	2.55	26.07

Table 4.5 The physical properties of the blue LEP inks

4.3.2 Results and discussion

Figure 4.11 shows the final morphologies of IJP blue LEP inks with different dot pitch, taken by the microscopy camera under UV light. From Figure 4.11(a), we can observe that the film printed with blue LEP in Phenetole at DP 28 and 48 do not have good homogeneous layer formations, even in the center of the printed area. While in Figure 4.11(b), because of the low boiling point of the 3- Methythiophene (115 ℃), the ink evaporate very fast during the printing process. Before the jetted drops merge together to form homogeneous layers, they already dried out and only form stripes. However, the films printed with blue LEP in Mesitylnene have very roughness surface, which are not be able to measure the accurate layer thickness by the Dektak.

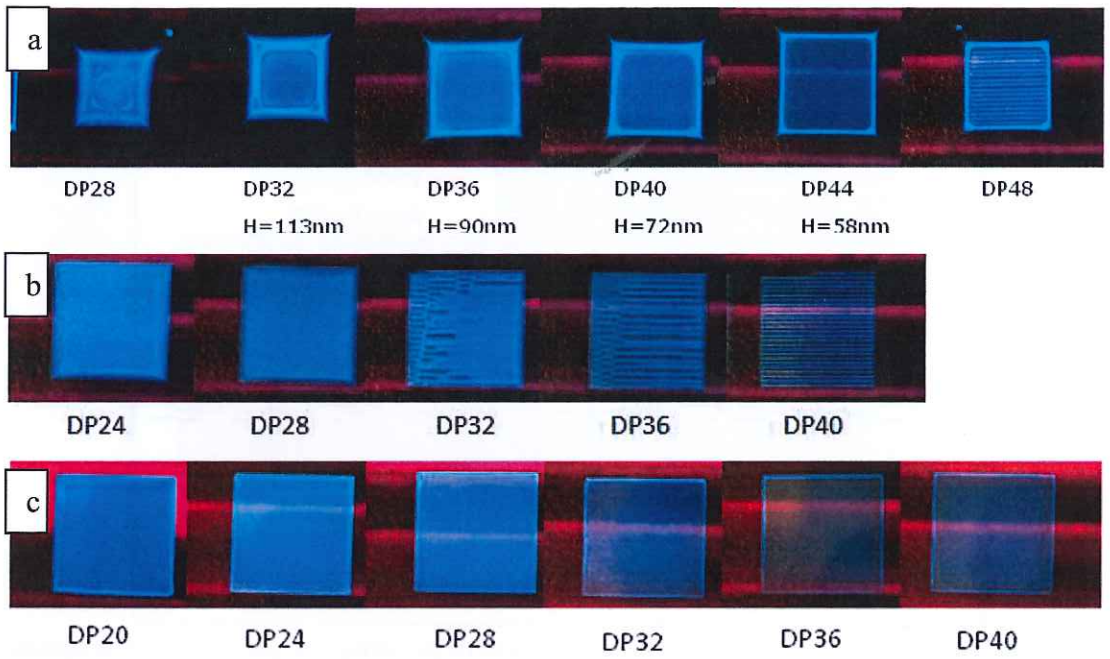

Figure 4.11 Final morphologies of IJP blue LEP inks with different DP on spin coated Pedot: PSS substrate under UV light and the measured layer thickness in the center, (a): blue LEP in Phenetole, for DP 28, the amount of the jetting ink is larger which needs longer drying time and the coffee stain effect is worse so no uniform layer formulates; for DP48, because the amount of the jetting ink is less and the droplets cannot merge to a homogeneous layer during the drying, only some stripes are form; (b): B-LEP in 3-Methythiophene, ink dried out during the printing and only form stripes due to the low boiling point of 3-Methythiophene ; (c):B-LEP in Mesitylene, the surface of the printed films are too rough to characterize the thickness.

Thus we only characterize the coffee stain of the films printed with 0.9wt% blue LEP in Phenetole form DP 32 to DP 44. The Dektak profilometer is used to characterize the surface coffee stain and the layer thickness. Then, the graphics of the relation between the DP and the coffee stain characterizations are plotted, as shown in Figure 4.12.

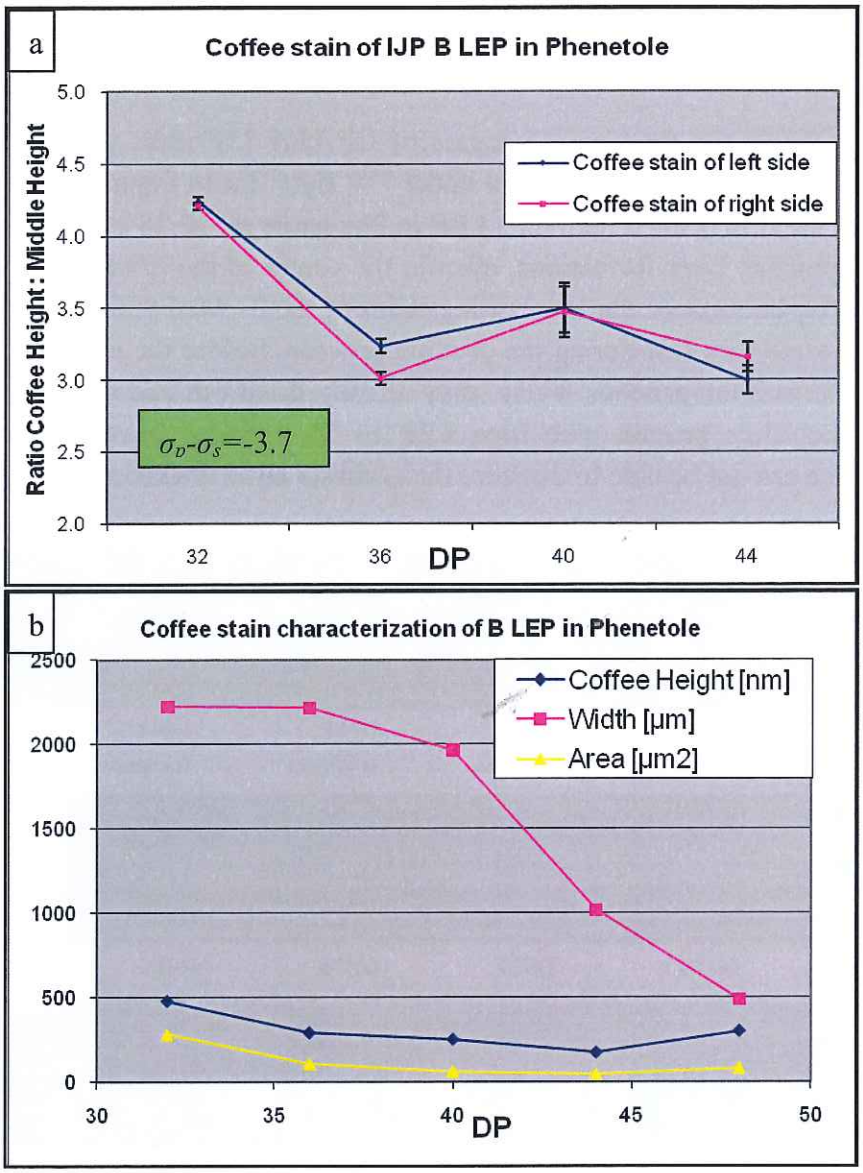

Figure 4.12 Coffee stain estimation as a function of printing dot pitch of 20mm square IJP ink of blue LEP in Phenetole (σ_p- σ_s= -3.7) on spin coated Pedot:PSS: (a) the ratio of coffee height over middle height decrease while the DP increases;(b) the height, width and area of the coffee stain decease while the DP increases.

From Figure 4.12 (a), we can find that the trend of the surface coffee stain changes as a function of dot pitch is the same as for the white LEP ink. The ratio of coffee height over middle height decreases with increasing DP, because the surface tension of the solvent is lower than the surface energy of the blue LEP material, and causes an inwards Marangoni flow. With a shorter evaporation time, the Marangoni effect has more effect on the coffee stain development, so the slope of the trend line is negative.

Due to the decreasing amount of the jetting ink for higher DP: the height, width and area of the coffee stain decrease when the dot pitch increases, as shown in Figure 4.12(b). In this case, the coffee stain is much wider while the height of the coffee stain is low because of the high surface tension.

4.4 Summary

In the chapter, it is observed that in the single solvent systems, for solutions which have homogeneous layer formation by ink-jet printing: if the solute surface tension is larger than the solvent's one, it reduces the coffee stain height but increases the width; if the solute surface tension is smaller than the solvent's one, it increases the coffee stain height but reduces the width, which means a very narrow coffee stain area; while if the solute surface tension is equal to the solvent's one, the coffee stain development can only be controlled by the evaporation rate.

In the case of no contact line pinning, more experiments need to be carried out in order to find the key factors of pinning.

5. Influence of the surface tension gradient in mixture solvents systems

After studying the influence of surface tension in a single solvent system, we move on to the mixture solvents system. According to the surface tension, the boiling point of the solvents and the surface energy of the white LEP polymer, we choose two mixture solvents systems. One system is the mixture of Veratrole and Mesitylene, and the other one is the mixture of Mesitylene and Indane. For each system, we use several different mixture ratios.

5.1 Experiments setup

We prepare the inks with LEP polymer in mixture solvents of different mixture ratios, and characterize the properties of the inks by the AMVn Automated Microviscometer and the KRÜSS Easy Drop standard. The details of the solvents and inks as well as the measured properties are shown in the Table 5.1 and 5.2.

Mixture of Veratrole and Mesitylene

0.9wt% White LEP in mixture of Veratrole and Mesitylene	Density [g/ml]	Viscosity 20°C [mPa.s]	Surface tension 20°C [mN/m]
Veratrole : Mesitylene = 20:80	0.90	4.66	28.86
Veratrole : Mesitylene = 40:60	0.94	5.87	28.91
Veratrole : Mesitylene = 60:40	0.99	8.51	30.90
Veratrole : Mesitylene = 80:20	1.03	13.59	32.02

Table 5.1 The density, viscosity and surface tension of the white LEP inks, formed by LEP dissolved in a mixture of Veratrole and Mesitylene in different ratios.

Mixture of Mesitylene and Indane

0.9wt% White LEP in mixture of Mesitylene and Indane	Density [g/ml]	Viscosity 20°C [mPa.s]	Surface tension 20°C [mN/m]
Mesitylene : Indane = 20:80	0.94	8.08	31.09
Mesitylene : Indane = 40:60	0.92	6.75	30.36
Mesitylene : Indane = 60:40	0.90	6.12	29.30
Mesitylene : Indane = 80:20	0.88	3.79	28.17

Table 5.2 The density, viscosity and surface tension of the white LEP inks, formed by LEP dissolved in a mixture of Mesitylene and Indane in different ratios.

In this section, we still choose the Dimatix Materials Printer to do the printing, because it is convenient to change the cartridge which is more suitable for this experiment. The Dimatix system jets 10 pL drops through up to 16 nozzles at 1kHz. For each ink, we print 20mm square on well cleaned soda-lime glass substrates or spin coating Pedot substrates using various the dot pitches (DP) of the printer. Then, the printed films are dried at 60°C on a hot plate with a 1mm spacer, and then annealed it at 180°C.

After preparing all the samples, microscopy photos is taken first to get the morphology of the layers, then the Dektak is used to get the surface profiles and the thickness of the dried layers.

5.2 Results and discussion

5.2.1 LEP in mixture of Veratrole and Mesitylene

After printing, we observe the following for the LEP inks that use a mixture solvent with a Veratrole weight percentage above 50%: during the drying process, the liquid shrink into a single drop at the center. Thus most of the polymer is deposited in the center instead of pinning at the contact line, as shown in Figure 5.1.

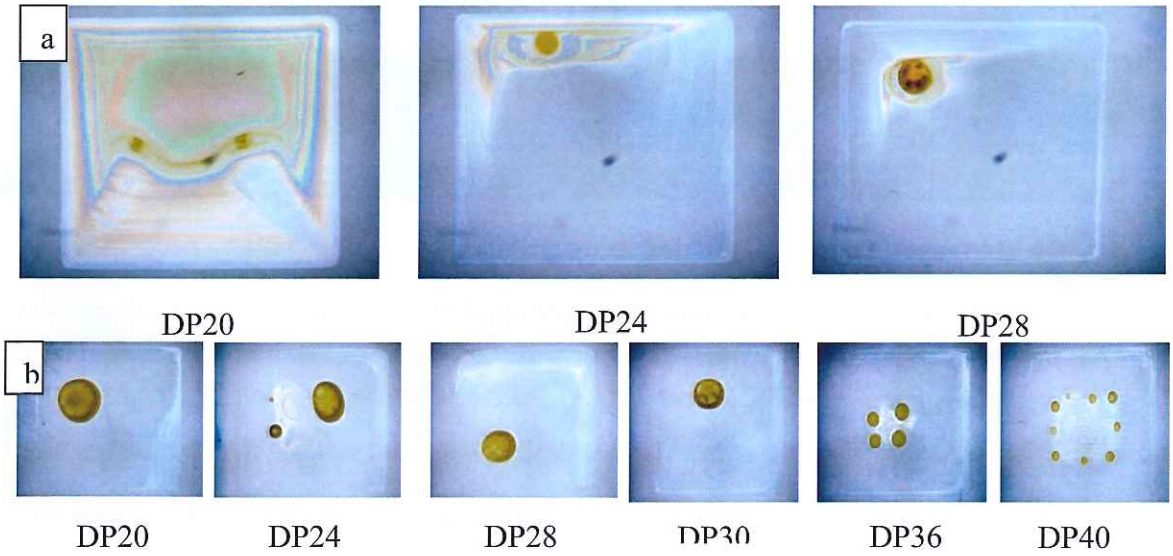

Figure 5.1 Final morphologies of LEP films, ink-jet printed using (a): 0.9wt% LEP in 80% Veratrole+20% Mesitylene (b): 0.9wt% LEP in 60% Veratrole+40% Mesitylene, with different DP on spin coating Pedot: PSS substrates by Dimatix Printer: no contact line pinning.

When printing with 0.9wt% LEP in 40% Veratrole+60% Mesitylene, the printed layers are inhomogeneous, as shown in Figure 5.2.

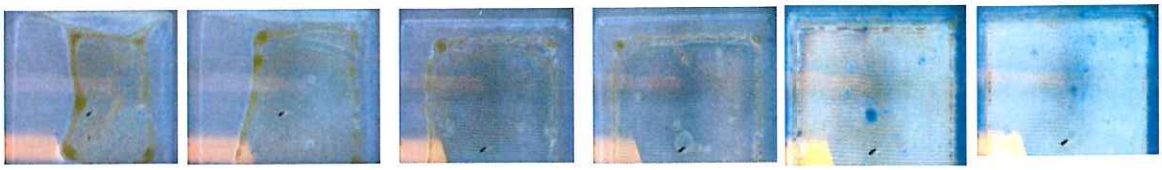

DP20 DP24 DP28 DP30 DP36 DP40

Figure 5.2 Final morphologies of LEP films, ink-jet printed using 0.9wt% LEP in 40% Veratrole+60% Mesitylene with different DP on spin coating Pedot:PSS substrates by Dimatix Printer: inhomogeneous layers.

Previously, in chapter 3, a mixture solvent of 60%Veratrole+40%Mesitylene was used in the Spectra Galaxy and LP 50 printer. However, from the results in Figure 1, it is found that this solvent cannot work with the Dimatix printer. So we use the Galaxy Printer to print with this ink, on both glass and Pedot substrates. In this case, quite homogeneous layers are formed, as shown in Figure 5.3.

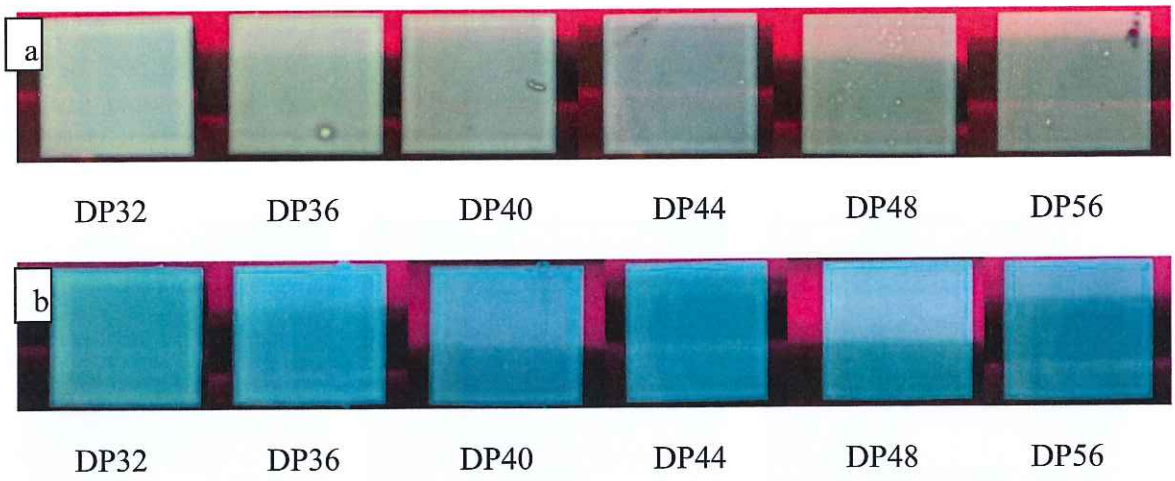

Figure 5.3 Microscopy images under UV light of LEP films, ink-jet printed using 0.9wt% LEP in 60% Veratrole+40% Mesitylene with different DP but same Line pitch 100μm on (a)spin coating Pedot:PSS substrate; (b) glass substrate by Galaxy Printer: very good layer formation.

The Dimatix system jets 10 pL drops through up to 16 nozzles at 1kHz, while the Spectra Galaxy system jets 50 pL drops through up to 256 nozzles. So the volume of the drops from the Spectra Galaxy printer is much larger than the volume of the drops from the Dimatix printer. Also, the required time to print the same pattern is much shorter: the Spectra Galaxy printer only needs one swath to print a 20 x 20mm film. While the Dimatix printer needs multiple swaths. The printer first jets from left to right to form a line, and then from up to down, all these drop lines will merge together and form a layer. From the results we find that the delays during the printing process and the drop volume of the print head have significant influence on the layer formation in the ink-jet printer process.

The solvents mixture of 60% Veratrole + 40% Mesitylene has a similar surface tension as the LEP polymer. From Figure 5.3 we can find a rectangular ring deposit at the edges, so we characterize this ring by the Dektak. The graphics from the Dektak data are shown in Figure 5.4.From this figure, it can be observed that with an increasing dot pitch, the ratio between the coffee height and the layer thickness is decreasing. Because of the boiling point of Mesitylene (166°C) is lower than the boiling point of Veratrole (207°C), the surface tension of the mixture solvents is increasing during the drying process. As mentioned in chapter 4, the surface energy of LEP polymer is 31mN/m, and the surface tension of the mixture solvents in room temperature is also around 31mN/m. Thus during drying the surface tension of the solvents becomes larger than the surface energy of the polymer, which forms an inwards Marangoni flow and decreases the height of the coffee stain. When the layer becomes thinner, the capillary force of the evaporation decreases, and the Marangoni flow plays the major role in the coffee stain development.

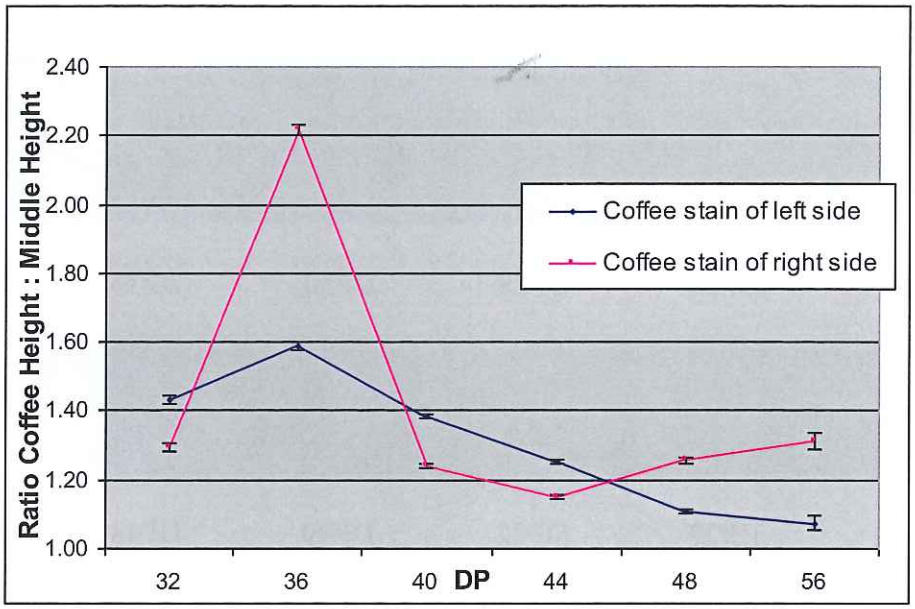

Figure 5.4 The ratio between coffee stain height and layer thickness as a function of the DP with 0.9wt% LEP in 60% Veratrole+40% Mesitylene on glass substrate.

5.2.2 LEP in mixture of Mesitylene and Indane

Since the mixture of Veratrole and Mesitylene is a system consisting of two solvents with a large difference in both boiling point and surface tension, another mixture is chosen that contains two solvents with a similar boiling point but a different surface tension. By changing the ratio of these two solvents, the surface tension of the mixture can be varied. Thus, a mixture of Mesitylene and Indane is chosen in this section.

For each ink, we also print 20mm square on spin coating Pedot:PSS substrates, with various the dot pitches of the printer. Then, the printed films are dried at 60°C on a hot plate with a 1mm spacer, followed by annealing at 180°C.

Figure 5.5 shows the microscope images of the morphologies of the printed films. From the images we find that all these inks have a good contact line pinning at the edges and form quite nice layers in the center, while coffee stain rings are still present at the edges.

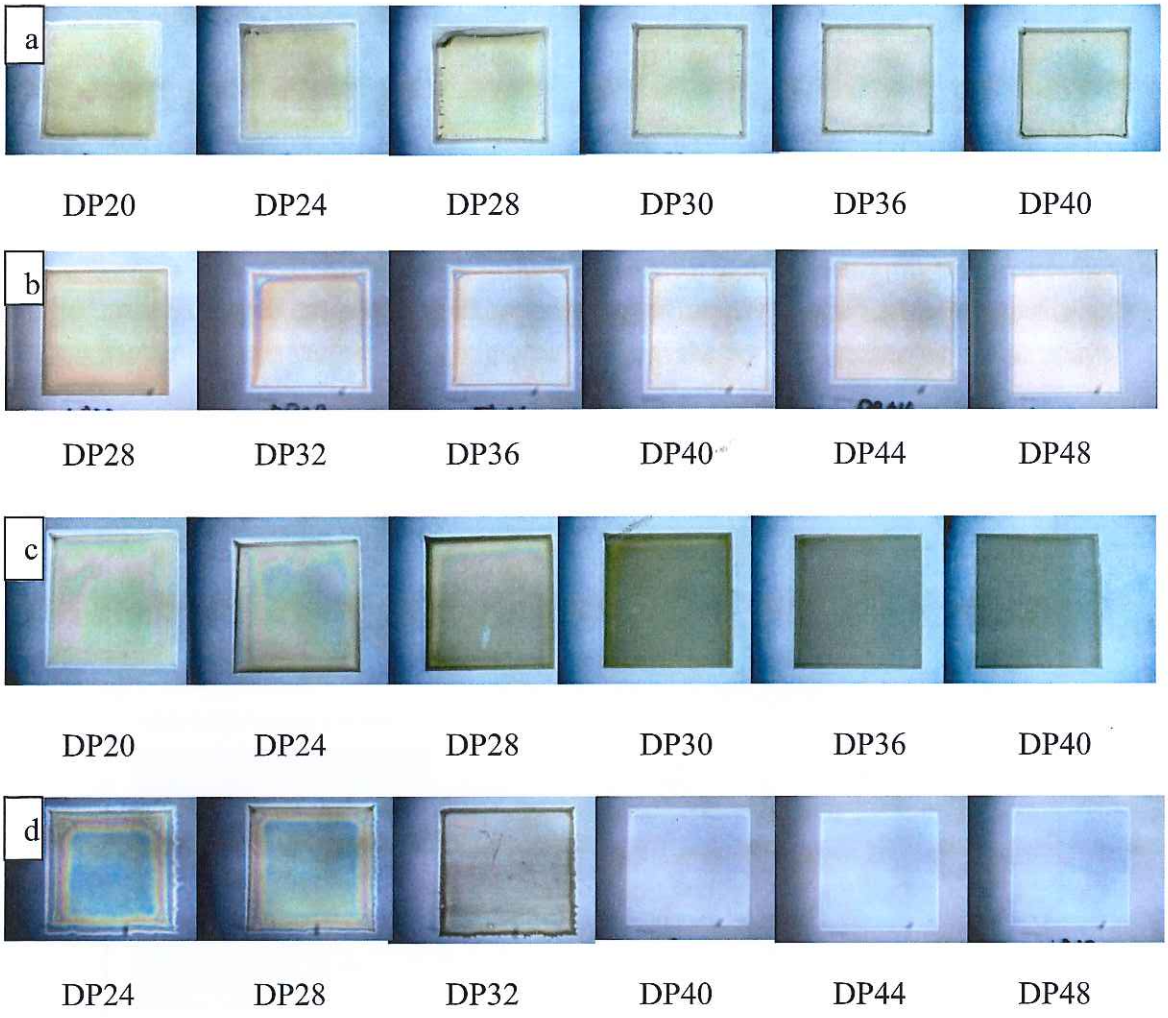

Figure 5.5 Final morphologies of LEP films, ink-jet printed with (a): 0.9wt% LEP in 80% Indane+20% Mesitylene; (b): 0.9wt% LEP in 60% Indane+40% Mesitylene; (c): 0.9wt% LEP in 40% Indane+60% Mesitylene; (d): 0.9wt% LEP in 20% Indane+80% Mesitylene with different DP on spin coating Pedot:PSS substrates by Dimatix Printer

In order to determine the effect of the surface tension and viscosity of the ink on the coffee stain development, we use the Dektak to characterize the surface profiles of the printed layer. We pick the films printed with DP 40 of four inks, and estimate the coffee stain of each ink from the average ratio of the coffee stain height and the height in the middle of a printed area as in the previous chapters.

The graphics in Figure 5.6 show how the surface tension and viscosity influence the surface coffee stain effect. The trend in Figure 5.6 suggests that an ink with a higher surface tension yields lower coffee stain, and also higher ink viscosity leads to lower coffee stain.

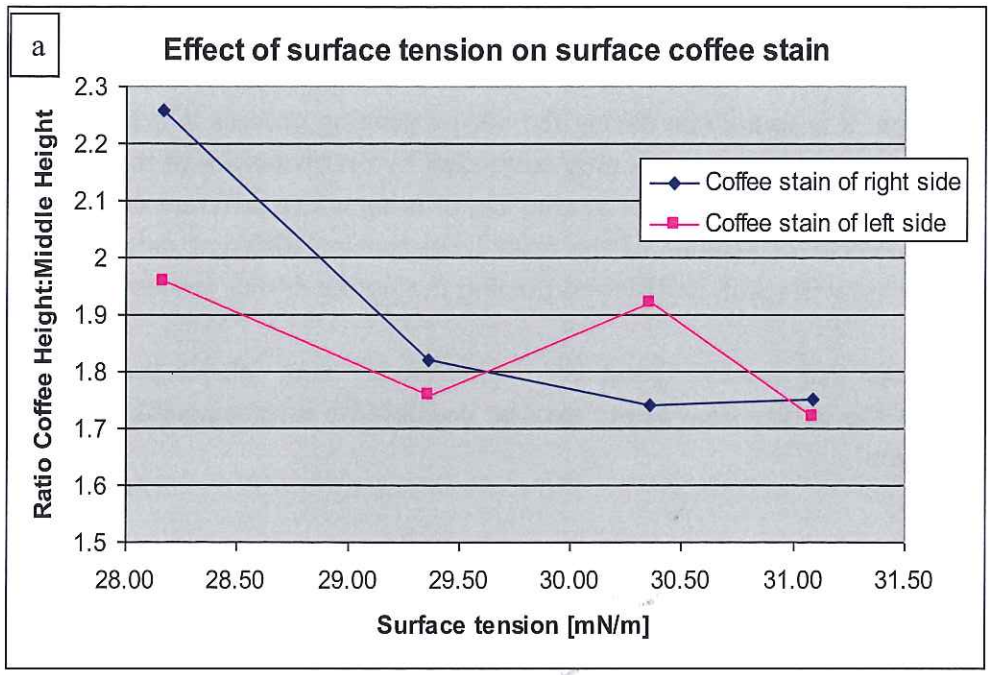

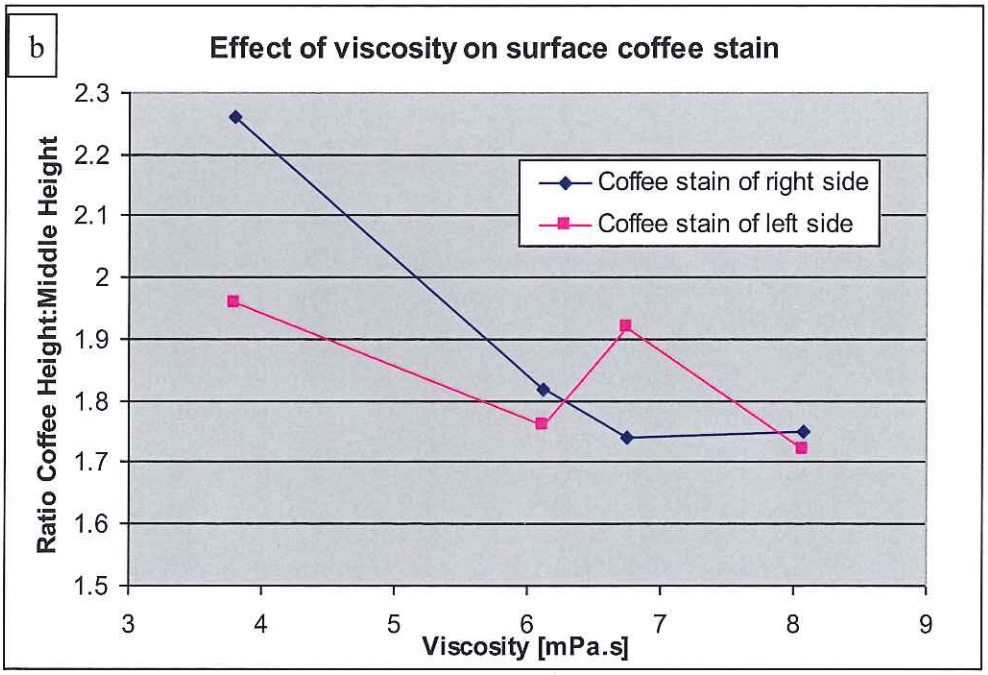

Figure 5.6 The coffee stain characterization of ink-jet printed LEP inks with different surface tensions and viscosities by the Dektak, (a): the relation between surface tension and coffee stain development; (b): the relation between viscosity and coffee stain development.

5.3 Summary

In this section, it is found that during the ink-jet printing process, whether an ink has contact line pinning or not, is not only controlled by the properties of the ink, but also by the properties of the Printer: for a same ink, printing with a different drop volume, or a different number of nozzles of the print head causing different delays during the printing process will result in different pinning during the drying process.

With the inks that achieve good layer formations using ink-jet printing, further reduction of the coffee stain effect may be possible by increasing ink viscosity and surface tension.

6. Device fabrication and performance characterization

Until now, we have done a lot of experiments to study the solvent selection and drying strategy optimization in order to produce a homogeneous film by ink-jet printing. Thus, at the end, we want to make some small molecular OLED devices by ink-jet printing with the optimal inks and drying strategy. And then, the current-luminance-voltage characteristics were measured by the IVL test platform to compare the performances of the SMOLED devices.

6.1 Fabrication of SMOLEDs

In this section, we made multi-layer SMOLED devices by ink-jet printing, the structure of each layer and the layer thickness are shown in Figure 6.1(a). Figure 6.1 (b) shows the schematic of the small substrate and the working area of the device.

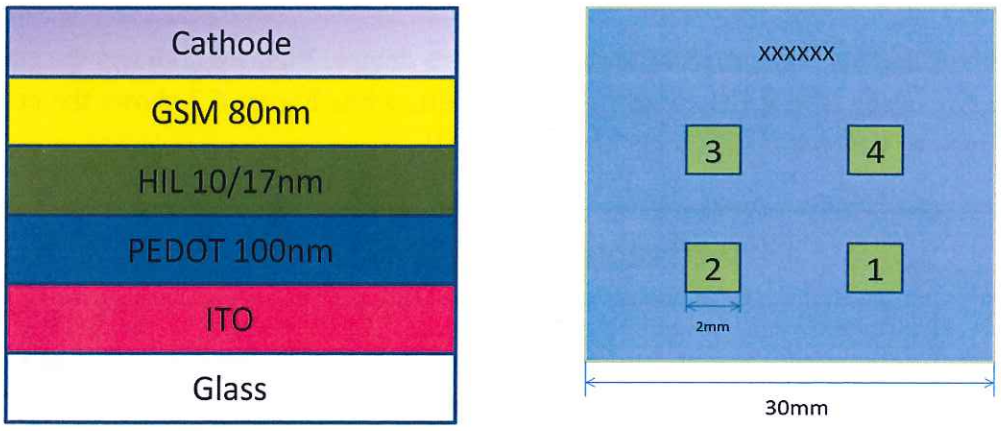

(a) (b)

Figure 6.1 (a).The structure of SMOLED device. IJP of three layers with PEDOT, HIL and GSM inks separately, and layer thickness of each layer; we vary the layer thickness of the HIL; (b). The schematic of the small substrate we used, it is a glass substrate with a size of 30 x30 mm and have already pre-deposit ITO layer on it. On each substrate we have four working devices with a size of 2x2mm, similar like the device shows in Figure 1.1(b).

The following is the process of the fabrication of the device:

- Clean the small ITO substrates
- Ink-jet printing a 15mm square of Pedot ink with the Galaxy printer, estimate layer thickness is 100nm, dried at 180 °C for 10 min.
- Ink-jet printing an 18mm square of HIL with the Dimatix printer, changing the DP to obtain two different layer thicknesses, estimate value is 17nm and 10nm, dried at

60°C with a spacer for 2 min, then annealing at 180°C for 1 hour inside the Glove Box.

- Ink-jet printing an 18mm square of GSM with the Dimatix printer, estimate layer thickness is 80nm, dried at 60°C with a spacer for 2 min, then annealing at 180°C for 10 min inside the Glove Box.
- Deposit Ba/Al as cathode

When finishing all the steps above, the SMOLED devices are for the performance characterization.

6.2 Device Performance

The current-voltage-luminance (IVL) characteristics are the common used method to characterize the performance of optical semiconductor components. The luminance is the luminous intensity per unit area projected in a given direction; and the SI unit is the candela per square meter (Cd/m^2) [5]. And the luminous intensity per ampere current pass through is the current efficiency of the device; the SI unit is the candela per ampere (Cd/A).

Figure 6.2 and 6.3 show the V-Eff curves of each device, Figure 6.2 shows the current efficiency of the SMOLEDs with 10nm-thick HIL while Figure 6.3 shows the current efficiency of the SMOLEDs with 17nm-thick HIL.

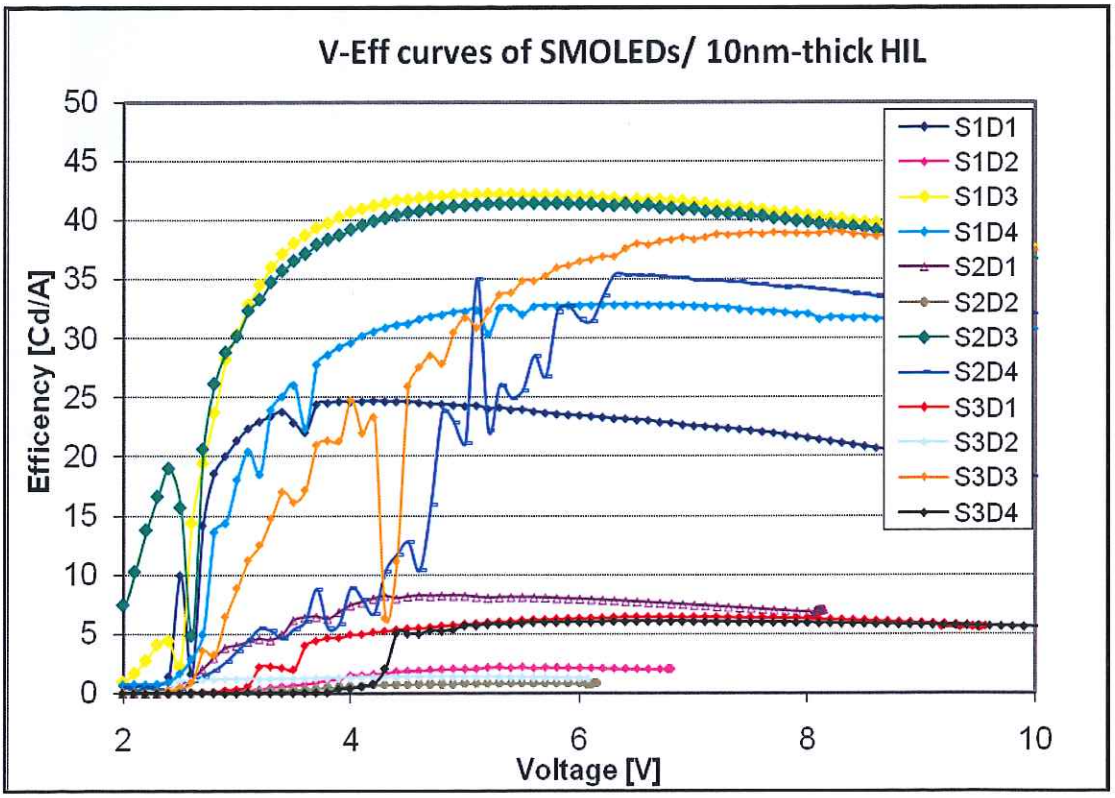

Figure 6.2 V-Eff curves of SMOLED devices with 10nm-thick HIL, the maximum current efficiency is 44.8 Cd/A.

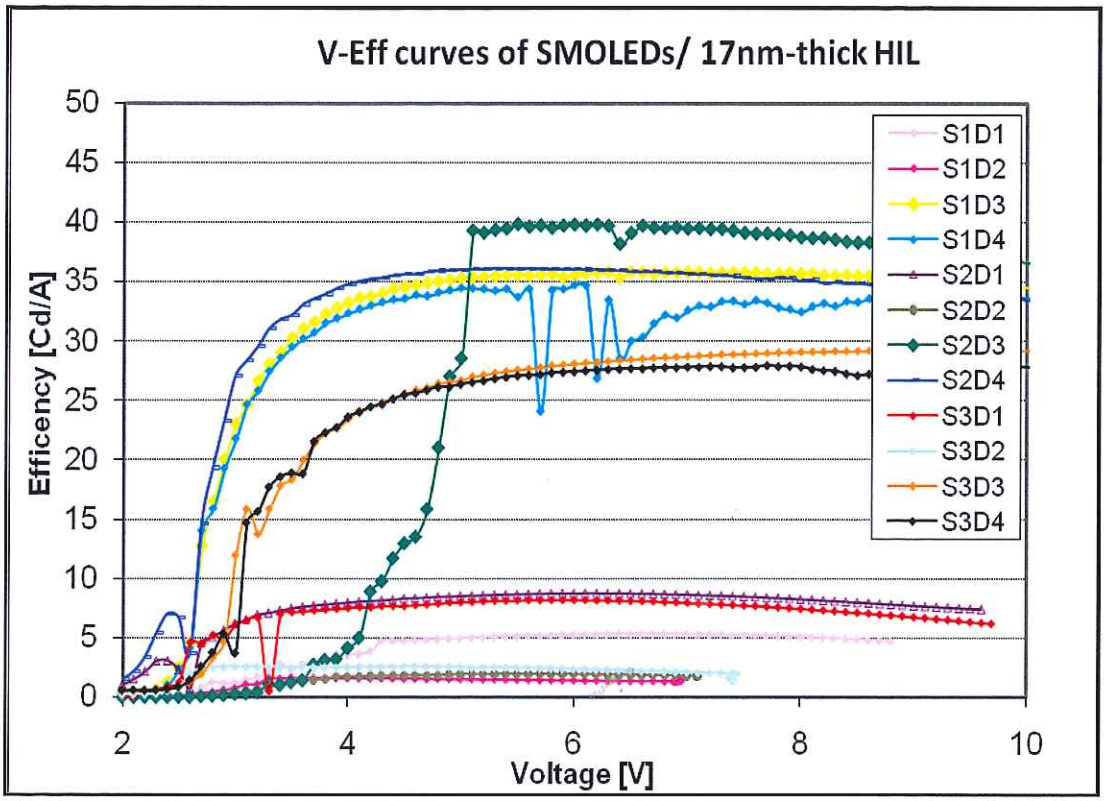

Figure 6.3 V-Eff curves of SMOLED devices with 17nm-thick HIL, the maximum current efficiency is 40.4 Cd/A.

From the curves shown in the Figure 6.2 and 6.3, it is found that, the devices in position 3 and 4 have much better performance compared to the devices in position 1 and 2. Because of the different delays during printing of multiple swathes with the Dimatix printer, it may influence the homogeneity of the film. But the accurate reasons which cause this phenomenon need further investigations.

Table 6.1 shows the summarized average and maximum values of all the devices efficiencies. From the values, we observed that devices with thinner HIL may have better performances than the one with a thicker HIL.

	SMOLED/10nm-thick HIL		SMOLED/17nm-thick HIL	
	Eff [Cd/A]	Voltage[V]	Eff [Cd/A]	Voltage[V]
Mean	18.81	5.27	15.53	5.83
SD	17.35	1.03	14.65	2.54
Max	44.8	4.0	40.4	6.7

Table 6.1 The averaged and maximum efficiencies of two types of devices are shown.

All the three function layers were processed by ink-jet printing, and the demonstrated current efficiencies are much better than expect, which confirms the good control of the coffee stain development and homogeneity of the layer formation.

7. Conclusion

The work summarized in this thesis has investigated the optimizations of the drying strategy and the solvent selection of the ink-jet printing process for producing OLED devices, in order to reduce the coffee stain effect and form homogeneous films. Plenty of experiments have been carried out to study the influences of the drying conditions and properties of the solvents on coffee stain development during the drying process, mainly related to the evaporation rate and the Marangoni effect.

For optimizing the drying strategy, different drying temperatures and methods have been tested for the purpose of reducing the coffee stain. As shown in Figure 3.6, the height of the coffee stain is increasing with an increasing drying temperature, while the width decreases as the drying temperature increases. Moreover, drying the printed substrate only with a spacer can considerably reduce the height and the width of the coffee stain by about 50%, compared to the cases that drying is done without a spacer or and with both a spacer and a cap. The optimal drying strategy is to dry at 80°C with a spacer. In this case, the ratio of coffee height over middle height, the width and the area of the coffee stain are at the minimum values. For some material which cannot stand high drying temperature, we also can use 60 °C which also reduces the coffee stain to an acceptable level.

For the selection of solvents for ink-jet printing, two systems have been tested: the single solvent system and the mixture solvents system. In the study of the single solvent system, we choose three types of materials: the white LEP, HIL and blue LEP materials. With each type of the material, we select solvents with different surface tensions compared to the solute, and form the inks. Due to the surface tension gradient, different Marangoni flows were discovered, which affects the coffee stain development. The interesting conclusion we observed is that for solutions which have homogeneous layer formation by ink-jet printing: if the solvent surface tension is higher than the solute's one, it reduces the coffee stain height but increases the width; if the solvent surface tension is lower than the solute's one, it increases the coffee stain height but reduces the width, which means a very narrow coffee stain area; while if the solvent surface tension is equal to the solute's one, the coffee stain development can only be controlled by the evaporation rate.

In addition, when ink-jet printing with HIL inks, the de-pinning phenomenon is found. During the drying process, the printed films do not have the contact line pinning at the edges, the material either shrinks into a small area and deposits there or retract into very small single drops and pin locally, instead of merging together and forming a uniform layer. We have some general analysis of this phenomenon, but more studies should be carried out to find the factors which control the pinning.

Furthermore, we worked with two mixture solvents systems: the mixture of Veratrole and Mesitylene, and the mixture of Mesitylene and Indane, both with several different

mixture ratios. With the inks consisting of Veratrole, no contact line pinning during the drying process with the Dimatix printer occurs. On the other hand, when ink-jet printing with the inks which consisting of a mixture of Mesitylene and Indane, uniform films are formed. The results from the coffee stain estimation suggest that further reduction of the coffee stain effect may be possible by increasing ink viscosity and surface tension.

At the end, we made some small molecular OLED devices by ink-jet printing with the optimal inks and drying strategy. After characterizing with IVL measurements, quite nice efficiency has been demonstrated, which confirms the good control of the coffee stain development and homogeneity of the layer formation.

8. Recommendation

By considering the results from this thesis, we find that some time inks do not have contact line pinning during the drying process. However, using the same ink with different printers, also results in a different pinning performance, for example, ink-jet printing with a certain ink can have good pinning and layer formation with the Galaxy printer, but it cannot pin with the Dimatix printer. So it would be better to further investigate about the factors involved in controlling of the pinning and how to predict if a solution will pin or not during the drying process.

Meanwhile, through all the experiments, we only reduced the coffee stain effect but have not eliminated it. Also, the study of the influence of the mixture solvents system is not sufficient. So it would be nice to carry out more experiments by choosing solvents with widely different properties, for instance, a solvent of low surface tension but high boiling point mix with a solvent of high surface tension but low boiling point. In addition, except dual solvents mixture system, it will be also interesting to do some researches of the trinal solvents mixture system.

Acknowledgements

This thesis work has been carried out in Holst Center/TNO in Eindhoven, The Netherlands. I would like to express my gratitude to everyone who supported and helped me to complete my work.

I am first of all grateful to my supervisor Dr. Maosheng Ren, thanks for giving me the chance to do my master thesis in TP1, where I really learned a lot and experienced a happy time. Thanks for all your inspiring ideas, direction and encouragement through my thesis work.

Harrie Gorter thanks for your kind and patient guidance and suggestions with the equipments in the cleanroom and data analysis, which helped me a lot in getting familiar with the lab work.

I wish to give my gratitude to all the people in TP1, for supporting me with my work and the friendly atmosphere you create during this period, especially Jasper Michels, Jorgen Sweelssen, Juliane Gabel and Charlotte Kjellander.

I would like to thank my examiner Shumin Wang, for improving and inspecting the written report.

Furthermore, my gratitude also goes to people from Miplaza, for helping me with the work in the cleanroom, especially Willy Wolter, Wendy Martam and Ton van den Biggelaar.

Finally I would like to thank my parents for supporting me with encouragement and understanding.

9. Literatures

1. http://baike.baidu.com/view/73395.htm#2 2011-07-25 entry.
2. http://tech.163.com/07/0525/10/3FB56ENG000926PT.html 2011-07-25 entry.
3. http://www.slashgear.com/oleds-blue-boost-cheaper-brighter-and-more-frugal-24 161297/#entrycontent 2011-07-25 entry.
4. http://en.wikipedia.org/wiki/Oled#cite_note-32 2011-04-15 entry.
5. Overview of OLED display technology; Homer Antoniadis, Ph.D. Product
6. Development Group Manager
7. http://expertscolumn.com/content/oled-advantages-and-disadvantages 2011-08-01 entry.
8. http://www.postech.ac.kr/ce/lamp/research3-3.html 2011-08-01 entry.
9. http://www.oled-display.net/oled-inkjet-printing 2011-08-02 entry.
10. Robert D.Deegan et al. Capillary flow as the cause of ring stains from dried liquid drops. July 1997.
11. Hanneke Gelderblom et al. How water droplets evaporate on a superhydrophobic substrate. September 2010.
12. http://en.wikipedia.org/wiki/Marangoni_effect 2011-04-10 entry
13. http://web.mit.edu/1.63/www/Lec-notes/Surfacetension/Lecture4.pdf 2010-11-24 entry
14. C. Poulard and P. Damman. Control of spreading and drying of a polymer solution from Marangoni flows. December 2007.
15. Eric Sultan et al. Evaporation of a thin film: diffusion of the vapour and Marangoni instabilities, May 2005.
16. Picknett, R. G.; Bexon, R. Evaporation of sessile or pendant drops in still air, J. Colloid Interface Sci. 1977, 61, 336-350

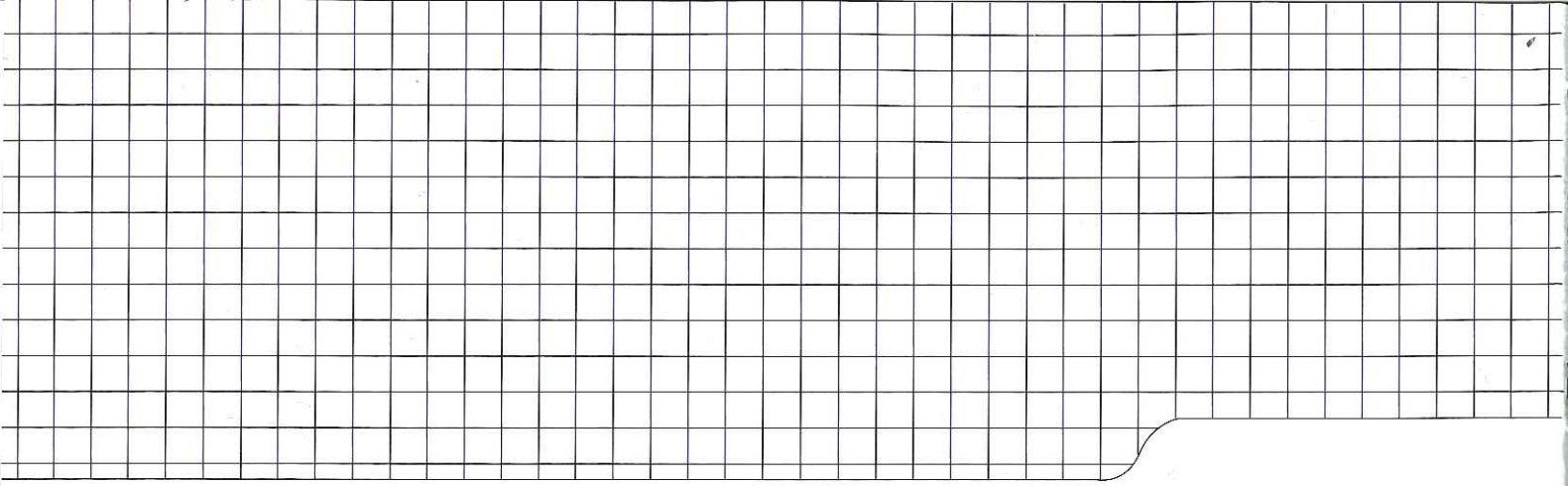

CHALMERS UNIVERSITY OF TECHNOLOGY
SE 412 96 Gothenburg, Sweden
Phone: + 46 - (0)31 772 10 00
Web: www.chalmers.se